Si-based MEMS Resonant Sensor: A Review from Microfabrication Perspective

Gulshan Kumar Verma[a], Kunal Mondal[b], Ankur Gupta[1a]

[a]*Department of Mechanical Engineering, Indian Institute of Technology Jodhpur, Jodhpur, 342037, Rajasthan, India*
[b]*Materials Science and Engineering Department, Idaho National Laboratory, Idaho Falls, 83415, ID, USA*

Abstract

With the technological advancement in micro-electro-mechanical systems (MEMS), microfabrication processes along with digital electronics together have opened novel avenues to the development of small-scale smart sensing devices capable of improved sensitivity with a lower cost of fabrication and relatively small power consumption. This article aims to provide the overview of the recent work carried out on the fabrication methodologies adopted to develop silicon based resonant sensors. A detailed discussion has been carried out to understand critical steps involved in the fabrication of the silicon-based MEMS resonator. Some challenges starting from the materials selection to the final phase of obtaining a compact MEMS resonator device for its fabrication have also been explored critically.

Keywords: MEMS, Fabrication, Design and packing of MEMS device, Application of MEMS

1. Introduction

Introduction to the silicon in the microsystems technology has brought up the revolution in the microfabrication field as number of devices can be conveniently fabricated on a single chip, which when realized as a comprehensive system can even accomplish complicated tasks. In general, micro-electro-mechanical systems (MEMS) is a physical system, which brings together

[1]*Corresponding author's email: ankurgupta@iitj.ac.in

components of both electrical and mechanical systems in a single platform [1]. Despite the fact that these MEMS fabrication technology comes out from the ICs fabrication techniques, but the test methods for both technologies have a prominent difference. The reason is the unique ability of these MEMS devices to respond to both electrical and non-electrical stimuli such as physical, biological, chemical and many more. The advancement in the technology enables us to reach out for building machinery or sub-structures at a very small range. Further reduction of the sizes of components, results in the nano-scale fabrications, such systems are called nano-electro-mechanical systems (NEMS). Plethora of their applications are being explored in automotive, space sector, healthcare and other domains, where human intervention for tracing the detection is difficult. Si based resonant sensors are such one of the widely explored systems. In a low–phase noise-based oscillation and stable–temperature-based applications, a higher Q–factor component with smaller form factor MEMS resonator is in demand so as to replace the quartz-based resonator. Many researchers have contributed in the development of Si-based capacitive resonator [2]. However, a relatively high dc voltage is required for operation of high–frequency based capacitive resonator, resulting in increasing difficulty in designing the low–voltage CMOS circuits [3]. Future of MEMS resonator is not limited to one application as it possess several advantages such as miniaturized level dimensions, lower power consumption and fabrication cost, low cost batch production, enhanced sensitivity, reproducibility, accuracy with smaller thermal constants and easy integration in the chip and many more [4]. Moreover, MEMS resonator with higher Q factor has a potential of replacing those off–chip, larger and incompatible CMOS components in wireless communication applications [5]. These are some of the reasons that attract researchers towards MEMS technology and for the same reason various MEMS resonator finds its application in the fields viz., Aerospace, Information technology, Medical related diagnosis, Bio-MEMS, Automobile, Robotics and many more [6, 7]. Significant research in MEMS resonator is generating huge MEMS market due to their high influence applications. These can significantly be used in applications such as sensing, timing and filtering and many more. In sensing applications, a given set of quantity can be measured with change in a resonant element [8], in timing applications, a resonant element is integrated with the electronics circuits to develop a high–quality signals [9], and in filtering applications, a resonant structure have filters that can be utilized for the RF wireless systems [10]. Various micro-electronics circuits can be distinguished

from MEMS resonator as these circuits have compact, rigid structures and are generally solid whereas MEMS resonator may have defects in the form of holes, channels and cavity. They may have membranes, structures like cantilever etc., below 80-100 µm which directly impact their manufacturing process as these structures cannot be machined by conventional process and therefore required specially designed fabrication techniques which involves etching and similar steps to free mechanical structures [11]. Considering the potential of this technology, this paper presents the summary of the recent work related to MEMS resonators and their micro–fabrication techniques. This will assist readers to have a better understanding of their performances along with the techniques and challenges behind the micro-manufacturing of MEMS resonators. The information gathered at one place may also be helpful for incoming researchers in designing integrated structures and devices mostly associated with the sensing and actuation.

2. Overview of Si-MEMS resonant sensors

2.1. Evolution and applications

The rise of micro-electronics-based devices can be traced back with the arrival of point contact transistor and junction transistor in 1947, which emerged as the technique for reducing sizes, portability and power requirement of devices. The discovery of Piezo-resistive effect phenomenon in Ge and Si in 1954, opened up a new era for the production of Ge and Si strain gauge, with 10 to 20 times higher gauge factor as compared to metal films [12]. The evolution in the MEMS technology was initiated with the two very important inventions of silicon semiconductor in the year 1959, which included Monolithic IC's chip by Fairchild semiconductor and MOSFET by Bell lab. With these inventions, researcher began to link the leeway of interaction and communication of silicon chips and MOSFETs with the external stimuli such as chemical, light, thermal, thereby opened the market for miniaturization of mechanical components and micro-machining technology [13, 14] The beginning for materialization of MEMS commercial products can be traced back in the mid-1990s [15]. Due to the continuous growth of MEMS techniques over the years, researcher are showing interest in its application in health- care sectors, few of them are medicine administrative systems, microvalve [16], micro-pumps, micro-fluidics [17], lab–on–chip (LOC), microscopic level instruments [18] and many more. The first kind of prototype related to the MEMS resonant sensor was reported wherein the RGT (Resonant Gate

Transistor) was introduced with cantilevered structure that acted as micro electro-static actuators [19]. In late 1980's LIGA technique were firstly introduced in the Germany, capable of making a component from electro-palatable substance [20]. To release micro-structures from single crystal Si and GaAs, a bulk micro-machining technique was demonstrated in 1992, called as Single Crystal Reactive Etching and Metallization (SCREAM) [21, 22]. The resonant frequency of silicon carbide (SiC) has shown better solution for the beams and cantilever structures as compared to its counterparts like Si and GaAs, and hence it gained attention to replace silicon for MEMS applications in extreme environment [23]. Due to the miniaturization of the sensor, MEMS devices can even be found in the space application, like MEMS louvers that is demonstrated in NASA satellite mission, which is used for thermal control of micro-satellites [24]. In order to significantly reduce the clean room fabrication cost for MEMS devices, a paper-based MEMS sensor was developed using a piezo-resistive principle. Performance of such paper based sensor can be improved by making its surface hydrophobic via silanization, which is generally used to minimize humidity effect on the sensor [25, 26].

With the advancement in the field of Internet of Things (IOT) technologies, the market for portable smart sensing device is rapidly attracting the researcher for the improvement in the design and fabrication of new materials for smart sensing and actuating purposes. IOT opens up a new ways in the analysis of real time collected data, its monitoring and its optimization that have a huge potential to build a smart surroundings [27]. The real time monitoring of aging civil structures and its control can increase the possibility of saving life of the people. This can be performed by introducing smart devices that are capable of dynamic response and detecting damages at the earliest [28]. Jena et al. has reported the summary of various embedded sensors based model for real-time structure health monitoring and failure detection in aircraft [29]. The only difference between the conventional integrated devices and MEMS based smart devices is that the later one utilized an intelligent component for digital data processing, analog to digital conversions, interfacing and many more. The output emerged from resonant sensors can be transmitted via radio-frequency (RF) signals, for which there are various wireless protocol such as Bluetooth, Wi-Fi, Zigbee, RFID, Z-wave and many more [30]. A wireless embedded MEMS piezoresistive based micro-cantilevered temperature sensor has been fabricated, which is capable of measuring soil moisture and temperature [31]. The advanced research for highly sensitive, cost effective smart sensor encouraged many

researchers to work in the field of effective sensors such as catalytic bead sensor [32], zinc oxide (ZnO) nano-bundles [33] and palladium (Pd) nano-structured platforms [34, 35] along with other resonant structures for gas detection. The idea of wireless self-generating power sensors were analyzed, where the energy from vibration of the civil structure are utilized for powering an accelerometer [36, 37].

2.2. Functional Aspects of MEMS Resonant Sensor

As it well known fact that the MEMS resonator consists of a vibrating component. Any change in the stresses or mass of the resonator via physical and chemical factors is thus converted to a resonance frequency of the vibrating component. Resonator with Si–material shows 100 times sensitivity in contrast to the standard available analog piezo-resistive transducers [38]. The quality and properties of the resonant device is function of its material therefore, a huge research is dedicated for searching suitable material. The alteration from the measured parameter to resonance frequency is done either via mass–loading of vibrating component or via change in internal force and stresses, which in turn changes the resonance frequency [39]. It has also been investigated that with the increase in the resonance frequency, stiffness of the vibrating–structure increases. The resolution and stability of the resonator also depend on the Q–factor, which is the ratio of total amount of energy stored in the vibrating structure to the equivalent sum of energy losses per cycle. A higher Q–factor is desirable for reducing the perturbing effect of micro–electronics, higher resolution, higher accuracy and stability [40].

There are various electrical means by which vibration of Si resonator can be measured such as capacitive, Piezo-resistive, magnetic [41], optical based detection techniques [42]. Flexible resonators are further categorized on the basis of vibration structure which are (i) the beam, (ii) the bridge and (iii) the diaphragm. Each vibration structures exhibit certain resonant modes of operation, and each mode further have its displacement pattern and Q–factor at resonance frequency. Any alteration in design of vibrating structures such as double or triple beam, leads to alter Q–factor results in increasing the vibration balancing. The Q–factor is directly correlated with damping, as different damping mechanisms limit the overall Q-factor [43]. Resonator working in a fluid such as gas will have a damping which results in reduction of Q–factor. Due to the presence of these gases around the surfaces, the vibration structures move in lateral as well as perpendicular direction. The Q–factor further depends on the properties of resonator material

such as purities, dislocations and many more. Low impurity single–crystal Si shows Q–factor of the order of 106, whereas high doped Si shows Q–factor of the order of 104 in vacuum [44]. The poly–crystalline material reported to have low Q value in contrast to the single–crystal material, explains by taking theoretical reference that perfect crystal have no losses [45]. The thermo–acoustic properties of the MEMS resonator can be altered by heavy doping of the Si substrate [46]. Various parameters can enhance the mechanical performances of a resonator, these includes Mode shape, amount of mode coupling, Q–factor, temperature sensitivity [47].

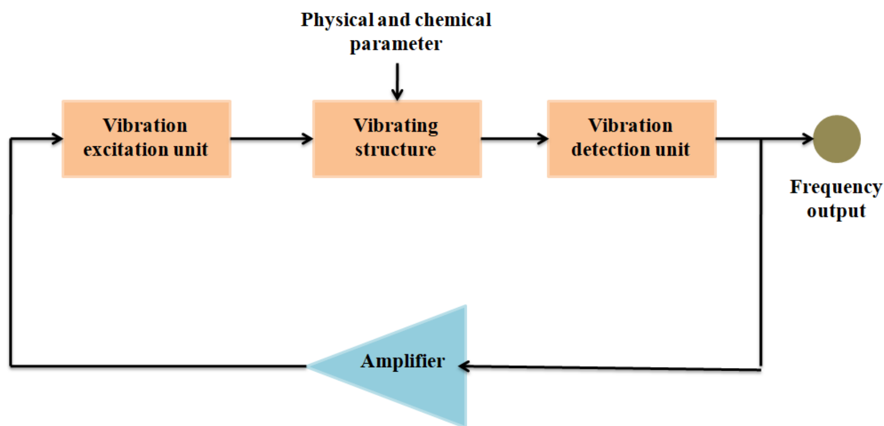

Figure 1: Schematic view of resonator sensor with feed–back mechanisms.

The Fig.1 shows the complete schematic of MEMS resonant sensor, which consists of, (i) the excitation unit, (ii) the resonator (iii) the detection unit and (iv) the feedback circuit. This feedback unit is used to maintain the desired resonance mode of operation [48]. The temperature sensitivity of the resonator is dependent, majorly on, resonant sensor material, their vibration mode of operation, bimetallic effects, and excitation and detection techniques. In silicon based resonator, the number of free charge carriers increases with doping and therefore, the temperature dependent resonance frequency is dominated by elastic constant such as young's modulus etc. [49]. So, by varying doping type, its concentration and altering the orientation of the resonator, temperature–coefficient of frequency (TCF) can be varied. Depositing a metallic layer had reportedly increased the efficiency of optical based excitation of vibrations and also suggested the coating of resonator with a material having a positive temperature–coefficient of young's modu-

lus to compensate temperature dependence of resonator. Research conducted for analyzing a contour–mode MEMS Si resonator, shows a high TCF in the range from -32.5 ppm/K to -23 ppm/K [50]. Electronics system requires filters for selecting the right signal and an oscillator for generating a precise reference frequency; these can be obtained by using a resonator especially in low–noise and low–power design. As the example, Clark et al. reported high-Q fabricated disk micro–resonator, micrograph of which is shown in the fig. 2 (a) [51]. Further Hajjam et al. developed thermally actuated high frequency silicon resonators through degenerate phosphorous doping as depicted in the fig. 2 (b) [52]. In another report, Si based thin film piezoelectric on silicon (TPoS) resonator was developed for enhanced power handling which is as shown in the fig. 3 [53].

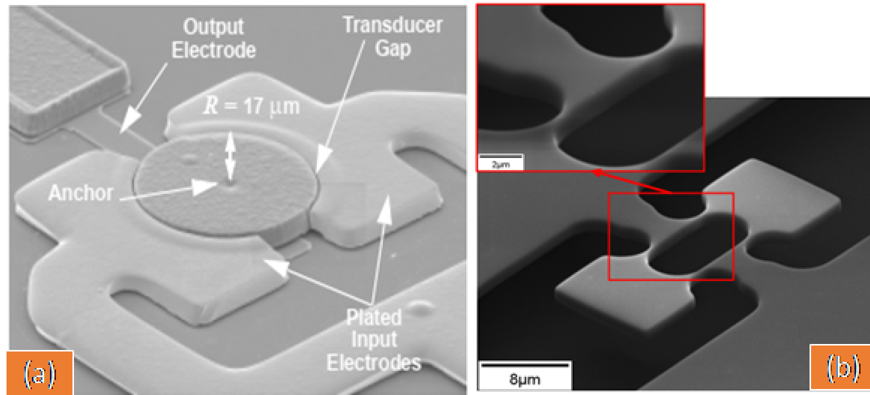

Figure 2: SEM image of a fabricated disk micro–resonator (left) [51] and SEM image of a piezo–resistive IBAR structure (right) [52]. [Reproduction of the figure with kind permission from [51, 52].

Below are the details of various resonance modes in Si resonant sensors:

Flexible model: Flexural–mode resonator can be given excitation in both plate and beam–structures modes. Both fixed and cantilever beams are commonly utilized beam–structures for sensing applications due to their simplicity in structure design and possibility of realizing associated proof masses [54]. Banerjee et al. investigated the resonance characteristic of a metallic micro–cantilever that has been fabricated by focused ion–beam technique, to demonstrate the improvement in the resonance amplitude of a vibrating–cantilever at a characteristic width [55]. Arlett et al. demonstrated the use of micro–cantilever to attain the lower temperature sensitivity by

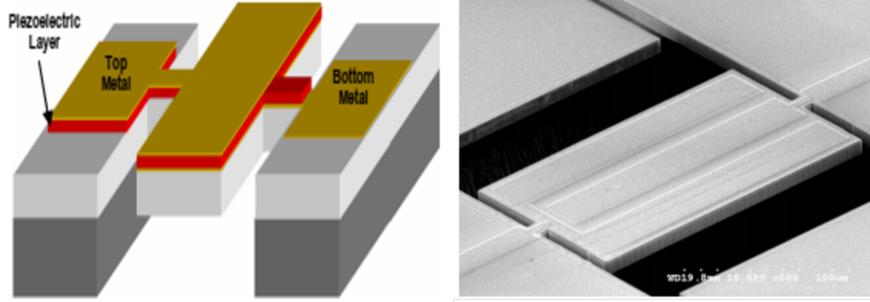

Figure 3: The schematic view (left) and SEM image (right) of AlN-on-Si TPoS resonator [53]. [Reproduction of the figure with kind permission from [53].]

electrically transducing micro–cantilever resonator with a force sensitivity of 235 aN/Hz1/2 at RT and 17 aN/Hz1/2 at temperature of 10K [56]. Burg et al. reported the change in the surface mass–loading condition in the order of 10-19 g/µm2 by suspended micro–fluidic channel resonator to demonstrate bio–molecular detection [57]. Canavese et al. presented a nano–machined holed resonating structure having micro–cantilever to improve resonance frequency with confirming up to 250% increase in the mass sensitivity [58].

Bulk mode: In Bulk–mode, deformation takes place due to planar expansions and contractions. Bulk–modes resonators have been previously reported for different shapes such as beams, circular–disks [59], rectangular–plates and square–plates [60]. Lin et al. confirmed the functional use of dual micro–resonator as a mass sensing system, with a sensitivity of 37 Hz/ng for bio–chemical sensing applications [61]. Tu et al. proposed an transduction setup which increases 67dB feed–through for a square–plate resonator, vibrating at 12 Hz with a feed–back consisting of both the capacitive and the piezo–resistive sensing units to cancel parasitic effects problems in micro–resonators [62]. Further, Kaajakari et al. demonstrated a 13.1 MHz bulk acoustic–mode Si resonator having a higher Q factor (Q = 130000) with a maximum drive level (P = 0.12 mW) at the hysteresis limit [63]. Ho et al. fabricated the piezoelectric on silicon based acoustic wave resonator as shown in the fig. 4 (a) [64]. Further lopez et al. developed VB-FBT micro disk resonator for the biomass sensing application as depicted in the fig. 4 (b) [65].

Other mode: Based on the propagation mode and its characteristics the acoustic wave resonator is further categorized into Bulk acoustic wave (BAW)

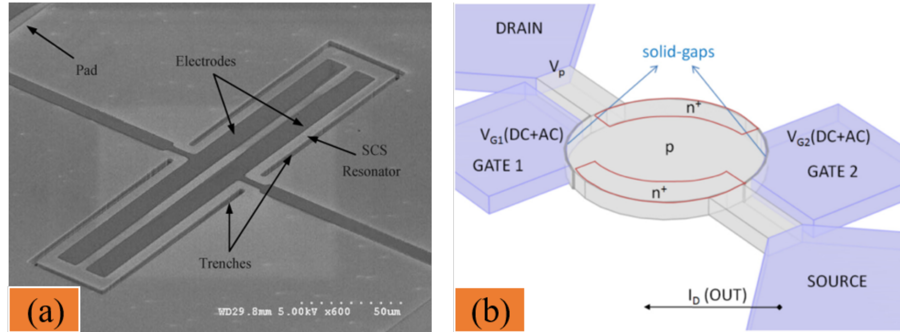

Figure 4: SEM image of a 240× 40×5 μm^3 piezo–electric on Si–bulk acoustic resonator [64] and Perspective–schematic view of the wine-glass mode disk–resonator [65] [Reproduction of the figures with kind permission from [64, 65]].

and Surface acoustic wave (SAW). The propagation of wave is occupying most of the volume of the bulk of material, this is bulk acoustic wave (BAW) [66] whereas in surface acoustic wave (SAW), a wave is traveling in interface of the solid and the air of device [67].

3. Fabrication methodologies for MEMS Resonant sensors

3.1. Material selection

The optimum level of performance for MEMS resonators are firmly dependent on the various material properties utilized. These material properties can be classified as mechanical, electrical, chemical, thermal etc. These MEMS resonators are often used in extreme and hard environment, a virtuous knowledge is progressively imperative in eliminating some of reasons of device failure through proper material selection, design and method of fabrication [68]. Mechanical properties can be further categories into three forms. First, an elastic property that helps in estimation of deflection response via application of forces. These elastic properties include modulus of elasticity and poison's ratio. Second property is internal stress, which are induced due to micro-structural changes and thermal mismatching and third property is mechanical fatigue, these are induces due to long run exposure of cyclic stresses, which may lead to the plastic deformation and change in the elastic constants that affects the sensitivity of MEMS resonator. Advancement of the materials has encouraged researchers to utilize various modern approach for selection criteria, one of them is Ashby approach, where the materials

are graded on the various performance indices based on its design, method of fabrication and application [69].

From a few decades, researchers have explored various kinds of substrate materials for the fabrication of MEMS device namely, silicon (Si)/ poly-silicon, silicon oxide (SiOx), glass & quartz substrate, silicon on insulator [70], silicon carbide (SiC) [71], diamond, shape memory alloys, GaAs and other group III & IV compound semiconductors. Some flexible substrate materials for the application of Bio-sensors and Bio-MEMS can be categorized into polymer, polyamide and paper based substrate, PET and PEN based plastic substrate, PDMS, polycarbonate and many more [72]. Single–crystalline material shows high level intrinsic Q–factors which enable its excellent resonating properties such as higher resolution, better accuracy and high repeatability. Whereas poly–crystalline Si material shows low level intrinsic Q–factors in contrast to single–crystalline Si, but possess good characteristics as these poly–Si resonant sensors structures can be fabricated in precise dimensions. Quartz is widely utilized material for the fabrication of resonant sensor as these are piezo–electric material; suitable candidate for the excitation and detection of vibration [73]. Bio-compatibility, chemical inertness, and hydrophilicity, as well as residual stress, etching sensitivity and selectivity along with the fabrication cost, are some of the parameters for when choosing a resonator material.

Over the years, single-crystal Si is economical and has widely been utilized for the manufacturing of MEMS resonator. They are mechanically stable and are ideal structure material with light weight, low mass density as compared to aluminum (2.3 g/cm3) and have a good modulus of elasticity, nearly twice as of steel (2×105 MPa). Si has low thermal expansion coefficient, nearly 8–10 times smaller than that of steel and aluminum respectively. Si can exist in all the three forms namely, crystalline, poly–crystalline and amorphous, with a crystal structure of diamond lattice. The electrical resistivity of Si is in the order of 10-3 to 104.5Ω-cm; therefore as per the need, Si can be made either conductor or insulator [74]. All these properties of Si make it suitable for mechanical, thermal, electrical integration in devices enhancing its suitability for extreme environmental applications.

3.2. Micro-machining Techniques

The fabrication of the Si based resonators can be performed using bulk micromachining, surface micromachining and LIGA technique [75]. The selective removal of material can be performed using wet and dry etching tech-

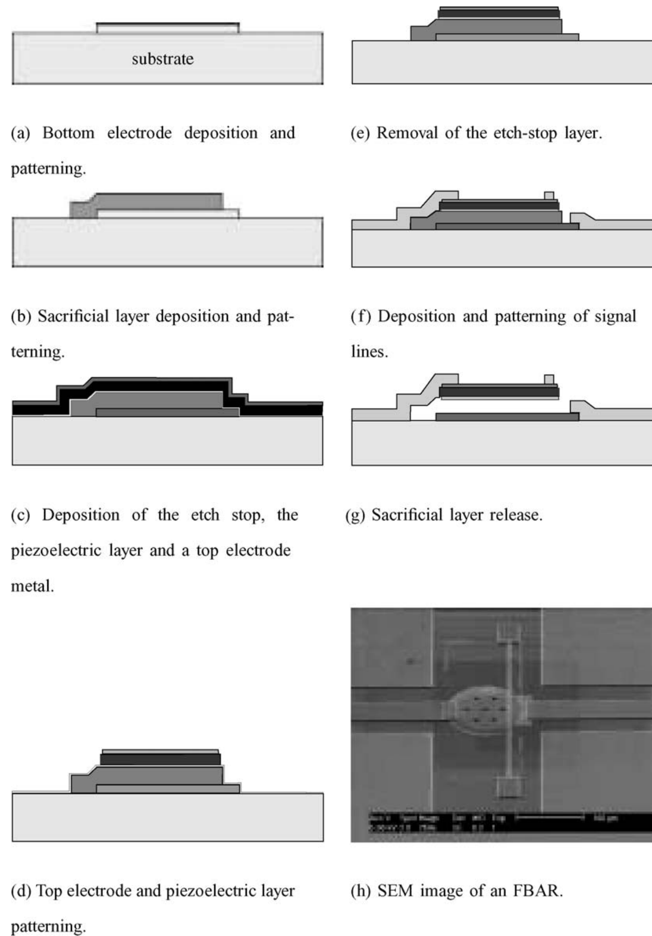

Figure 5: Process flow of the surface micro–machined film bulk acoustic resonator (a to g) with SEM image (h) [78]. (Reprinted with permission from [78]).

nique. In this process, Si wafer with a crystal orientation of 100 and 110 is used to produce simple micro-structures such as membranes, diaphragms, square mass, channels and cantilever [76]. Typically the resonator fabrication consist of sacrificial layer deposition, patterning of contact and structure layer, etching of sacrificial layer, consequently releases a micro-structure layer in surface micro-machining techniques [77]. A mechanical property of single-crystal Si substrate such as modulus of elasticity and poison's ratio can be obtained repeatedly in contrast to deposited sacrificial film of poly-Si whose properties depends mainly on processing conditions. For the same performance, micro-structures formed by surface micro-machining technique are

smaller in contrast to bulk micro-machining technique. Adding impurities to Si based devices can leads to micro-structures curvature and buckling; that can affect the resonator performances [79]. The surface-chemical alteration method can lower the friction and enhances the wear life of Si as a structure material [80]. A 10µm–thick resonator microstructure is fabricated with surface microstructure a deposited polysilicon film [81]. The summary of the various parameter involved in the fabrication of surface and bulk micromachining is presented in the table 1. Pan et al. developed electrostatically tunable film based on a bulk acoustic resonator using surface micromachined technique and the various steps involved in the fabrication is shown in the fig. 5 [78]. In another report, the fabrication of the low stress CMOS on Silicon carbide substrate as shown in the fig. 6 [82].

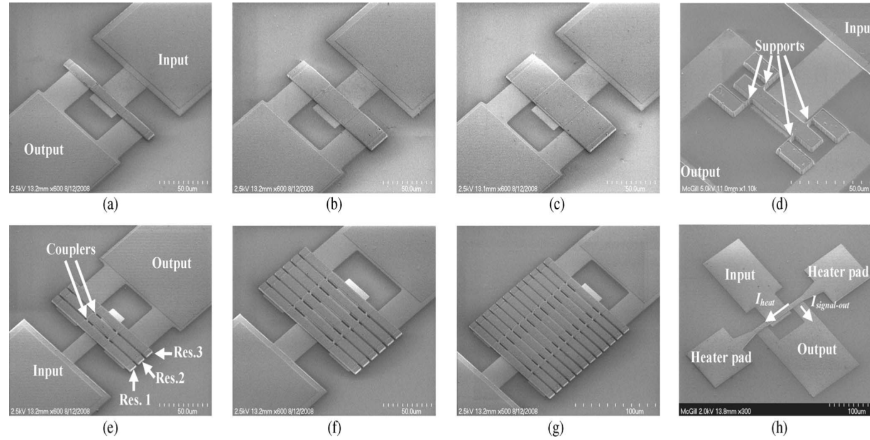

Figure 6: SEM image [(a), (b), and (c)] of fabricated c-c beam resonators with dimension 10–μm, 25–μm, 40–μm wide and 45-μm-long (d) f-f beam resonator a 10-μm wide and 64-μm long [(e), (f), and (g)] resonator arrays consisting of 3, 6, and12 beam (h) SEM image of a resonator with an integrated–heater [82]. (Reprinted with permission from [82])

Zachary *et al*. [84] used surface micromachining techniques for the fabrication of Si based resonator. The first step is to dope the substrate to make an actuation electrode as conductive. A 1 μm thick oxide layer is produced and patterned via UV lithography process, followed by BHF etching. The second step involves the deposition of a thin LPCVD silicon nitride layer 300 nm, followed by a thick (4–5 μm) oxide layer deposition via PECVD process. Finally, the oxide layer is patterned using UV lithography techniques and a 300 nm Al deposition is performed. The third step involves the deposition of

Table 1: Performance parameter of surface and bulk micromachining [83]

Performance Parameter for MEMS Resonator	**Surface micro-machining**	**Bulk micro-machining**
Mechanical properties	Good	Superior
Dimensional control	Superior	Good
CMOS integration	Good	Normal
Packaging parameter	Normal	Normal
Size and shape	Smaller	Small
Cost	Normal	Good

200 nm thin LPCVD polysilicon layer. The fourth step involves deposition and patterning of a thick (1-2 μm) LPCVD silicon nitrate layer.Figure 7, shows the various steps involved in the fabrication of micro-resonator structure [84].

Rusch *et al*. [85] presents a fabrication of the MEMS microstructure of dielectric resonators for electronic frequency tuning with low Q factor. The fabrication of microstructure is presented with high aspect ratio and high accuracy of the LIGA process. Bijari et al. demonstrated a novel approach to fabricate a low-cost UV-LIGA technology for the manufacturing of resonator with three simple steps for obtaining high aspect ratio with 20 with 3 µm of gap. Fig. 8, shows the image of LIGA processed structure along with a SEM view of fabricated MZI- ring capacitive loading. Another report involves the fabrication steps for obtaining high aspect ratio micro ring resonator along with SEM image as shown in fig. 9 and fig. 10 [86].

Kim *et al*. [87] proposed a fabrication method using modified LIGA for the manufacturing of the micro-injection mold. The modified LIGA reflow process is performed in three steps; namely lithography, thermal reflow and electroplating process. For obtaining the very strong microstructures, electrodeposition of Ni-Co, Ni-W and Co-W used the pulse plating technique so as to prevent the aggregation of unwanted products at the bottom [88].

Micro-fabrication of Si based resonator is performed in a specialized environment where the level of particle and metallic contaminations are in controllable state. The microfabrication techniques are divided into two major categories namely, hard technologies for Si based devices and a soft technology for elastomeric materials application. These soft technologies are preferred due to their easy, rapid and low-cost micro-fabrication processes [89]. The process of micro-fabrication starts with the cleaning of wafer via Pi-

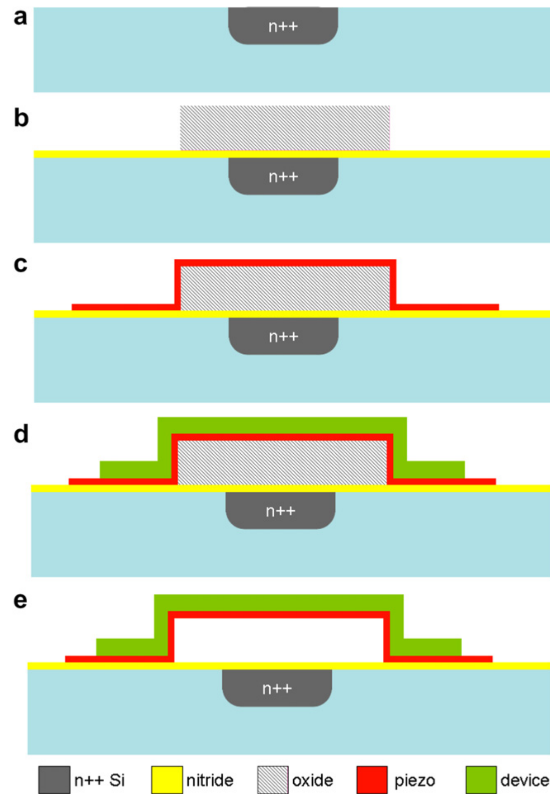

Figure 7: Fabrication sequence of the micro-resonators structures with integrated electrostatic actuation and piezoresistive readout. [84]. (Reprinted with permission from [84])

ranha clean, RCA–I and RCA–II process (RCA is an acronym for Radio Co-operation of American) [90]. These cleaning steps not only prepare a wafer for the subsequent processes but also remove out any particle and metallic contamination from wafer that can affects the devices performance.

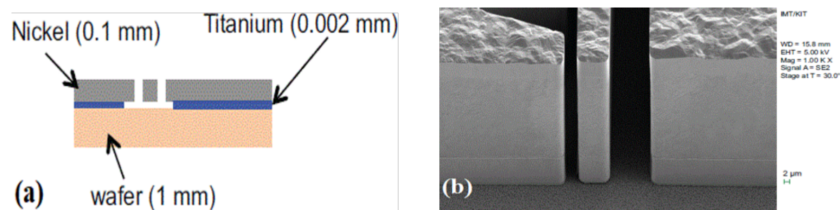

Figure 8: (a) Layer stack-up of LIGA-processed structure; b) SEM image of movable beam for tuning MZI-ring capacitive loading. [85] (Reprinted with permission from [85])

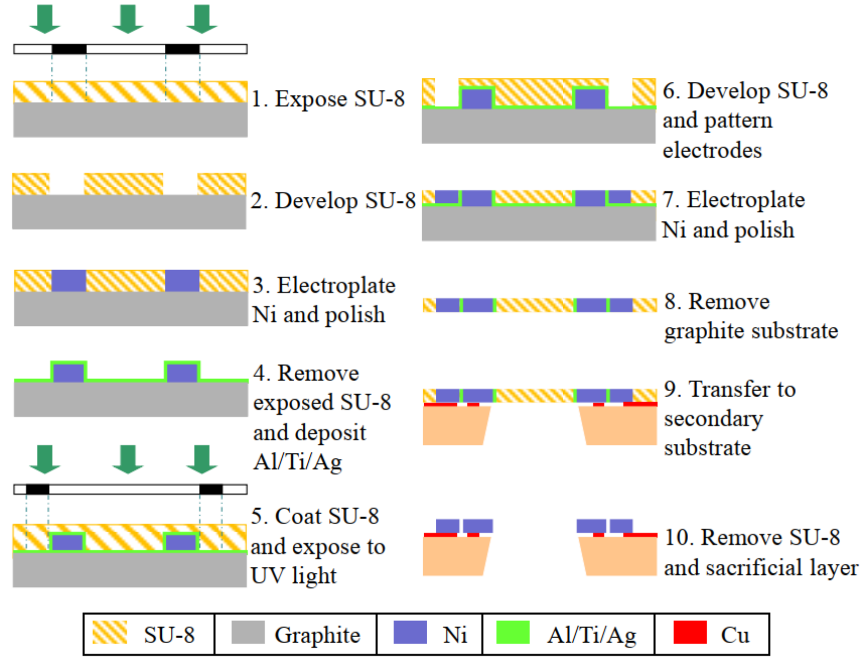

Figure 9: Schematic diagram of ring filters using UV-LIGA technology [86]. (Reprinted with permission from [86])

The next steps in the fabrication are discussed in the following sub-sections.

3.2.1. Deposition Process

The method of deposition of the thin films on Si wafer can be performed by the application of a protective layer, which can assist to alter and protect the substrate surface by enhancing its properties like resistance to wear, corrosion [91]. There are various applications of these thin films coating ranging from electrical, electronic materials, sensors, biomedical related devices, aerospace, automobile industry and many more. Deposition of aluminum nitride (AIN) is suitable for BAW resonators as it is chemically stable and having a bonding energy of about 11.5 eV, better thermally conductivity with low temperature–coefficient. Also it does not contain harmful element that can cause contamination of device [92]. Gupta et al. fabricated a portable biosensor with a nano-composite based film containing ZnO–Au–NPO; which enables a fast sensing dip-stick model via a coated-flat chip which refines the detection sensitivity up to 1 CFU/mL [93]. The reason for presence of mechanical stress in the deposited film can be explain by two strands.

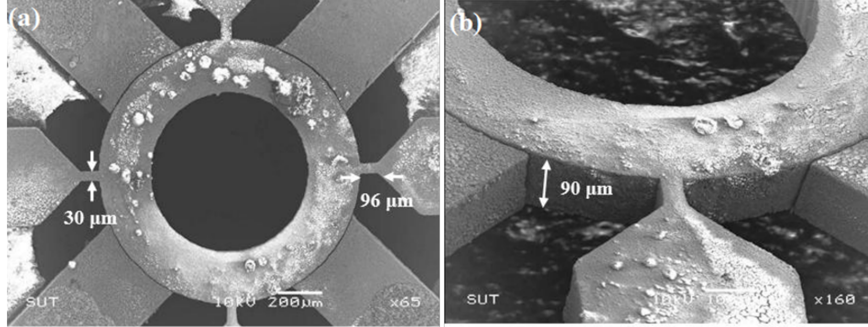

Figure 10: SEM images of the micromechanical ring resonator [86]. (Reprinted with permission from [86])

The first one is due to the presence of different coefficient of thermal expansion between deposited film and substrate material, and secondly; due to surface imperfections. Hara et al. deposited an AlN film using RF magnetron reactive sputtering technique that gives lower process temperature than CVD [94]. Gupta et al. reported an optical sensing work with a surface coating of porous polymer-film; a reduction in surface-roughness up to 33 nm is obtained in contrast to the 235 nm surface-roughness of uncoated surfaces, which in turns reduces 27.42% relative transmission losses [95]. Prior to the deposition step, a high temperature baking step is performed to breaks down the SiO2 layer and allows the Si to reflow and smooth the surface features and finally leave the Si with a low–surface roughness [96].

Table 2: Various deposition techniques used in micro-fabrication of MEMS resonant sensors.

Deposition techniques	**Sub-categories**
Chemical-reaction	Chemical vapor deposition (CVD), Electroplating, and Epitaxy
Physical-deposition	Evaporation and Sputtering
Spin-coating	Spin coating and spraying

The use of sputtering process has been reported for the film deposition of aluminum (Al), silver (Ag), gold (Au), and gold-palladium (Au-Pd) on zinc oxide (ZnO) nano-structure which is fabricated vertically on Si substrate for enhancing the efficiency of remediation of industrial based dyes [97]. These are further classified as a reactive, triode and magnetron sputtering.

Hoche et al. investigated a synthesis protocol of two thin film coating of Al2O3 and Cr-N by using PVD and experienced that the rate of deposition is reducing as the deposition time increases due to the effect of back sputtering [98]. Contreras et al. utilized magnetron sputtering technique, to synthesis TiAlN–TaN layers and observed that it shows stronger relation towards mechanical properties as the critical load capabilities increases [99]. Magnetron sputtering technique is known as a highly preferred technique due to high resistance to wear and low coefficient of friction but yield lower ionic flux and lower ionic energies. These types of problems associated with magneto sputtering can be rectified by pulsed-DC sputtering technique. In pulsed-DC technique a frequency of 25–350 kHz was utilized to alternating the polarity of the source target so as to provide excitation to the target atoms. The relationship between increasing ion bombardment w.r.t unbalanced–magnetic field is been investigated, which revealed the improvement of Al-N film deposition [100]. For probing the effect of the sputtering rate and presences of stresses on deposited film, an investigation on various parameters were carried out. Ababneh et al. reported that; with the increase in the concentration of sputtering powder and decrease in the sputtering pressure level, the positive charged ion with high kinetic energy will be accelerated towards the target, which in turn increases the momentum transfer-rate resulting in higher rate of sputtering [101]. Increase in the concentration of N2 gas results in the decrease of sputtering rate when nitrogen gas is utilized as sputter agent. Chaudhry et al. fabricated a thin film consisting of TiN–Ti on p-type silicon substrate by using magnetron sputtering and observed that it improves chemical and thermal and electro-chemical stability [102].

CVD being another method is used for the deposition of films using chemical reaction [103]. For the synthesis of thick dielectric (like SiN), Atmospheric Pressure chemical vapor deposition is used, as it has advantage of high deposition rate. The low-pressure chemical vapor deposition (LPCVD) process has advantage that it can deposit thin films on both sides of the wafer surface, but with relatively slow rate and higher deposition temperature. It is used to deposit better uniform films of SiO_2, W, SiN, SiC and High Temp Oxide (HTO). Naing et al. has demonstrated various steps involved for fabrication of disk resonator for depositing 2-3 μm–thick resonator structure of POCl3 doped poly–Si via CVD deposition technique [104]. The dielectric constant of low temp oxide (LTO) in contrast to thermal oxidation is about 4.3, due to its lower temperature deposition, that increased its dielectric strength is about 80% [105]. Serra et al. has fabricated the Si–resonators by

using bulk–micromachining mechanism. LPCVD thermal–oxide layers with a thickness of 100-300 nm are grown at the temperature of 1100 °C [106]. Another method used to deposit SiN as a passivation layer, is Plasma enhanced chemical vapor deposition (PECVD) which utilizes low temperature to produce film (200–400 °C), but low temperature also reduces the surface mobility of the reactant, which results in the formation of amorphous thin films [107]. By a simple modification in the deposition indices such as applied pressure and gases flow-rate, there is a possibility of controlling stresses in the deposited films via PECVD [108]. Furthermore, Joachim *et al*. [109] demonstrated an addition of material to MEMS structures by selective deposition of polysilicon in order to explore a new way of trying to compensate for varying micro fabrication system parameters. The electrical heating of the MEMS resonator is performed in a 25 °C in the presence of silane gas to enable the decomposition process and it was found that the rate of deposition for polysilicon is three times faster in contrast to LPCVD.

3.3. Lithography

It is well known that the designed pattern is transferred onto the wafer using a technique called lithography. In order to transfer this pattern, a photo resist material is applied on the top of wafer and is been selectively exposure to an illuminating source such as UV light. Kumar et al. proposed a laser assisted micro-machining techniques for manufacturing of these hard-masks through a micro-machined Al shadow-mask [110]. The minimum feature sizes that can be obtained are up to 10 μm [111]. Yan et al. proposed three photo–lithographic steps to release the resonator structure and a 140 μm pressure sensitive diaphragm was etched on Si handle layer by DRIE technique with the help of patterned PR mask [112]. Once the design pattern is transferred, the resist is usually stripped off. This is important step as the resist is incompatible with other micro-fabrication steps and cannot sustain high temperature [113]. The accuracy of MEMS fabrication depends on these photo-masks accuracies. Highly sophisticated machineries are involved with precisely operation for fabrication of these photo masks enhances its cost [114]. Deshpande *et al*. [115] designed and fabricated a piezoelectric based MEMS contour mode resonator with ZnO as material. The micro fabrication starts with the deposition of SiO2 layer on the top of p-type Si wafer via thermal wet oxidation process with the operating temperature of 1000 °C for 3 hr. Followed by the deposition of ZnO layer of 250 nm using 100 watts RF power sputtering. Electron beam lithography technique has

further been explored for the locating alignment marks which begins with the coating of PMMA resist via spin coating at 3000 rpm for 30 s. Next step is the deposition of Cr/Au layer of 10 nm and 80 nm respectively. The deposition of PPR (positive photo resist) takes place for the creation of cavity via optical lithography. Fig. 11 shows the SEM view of the fabricated MEMS resonator. Ferran *et al.* [116] proposed three lithographic steps for the fabrication of a RF-MEMS resonator. 1 μm thick Al layer is deposited using sputtering along with the patterning of 650 μm thick glass as substrate to determine the structure for coplanar waveguide. Followed by the deposition of 3 μm thick sacrificial PR layer for defining and patterning the anchoring regions of resonator before a second Al layer is deposited. Finally, the PR is removed in order to defines and release the resonator MEMS beams.

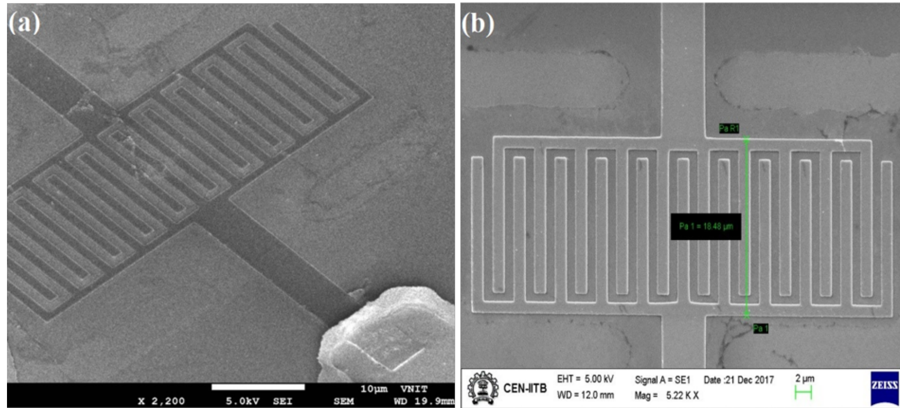

Figure 11: SEM view of micromachined contour–mode resonator. (a) Cross-section views. (b) Top views. [115] (Reprinted with permission from [115]).

Luo et al. proposed the fabrication steps of the Si–based MEMS resonators on a 4–inch SOI wafer by involving only two photo–lithographic steps, for creating the resonant structure. A 120–μm pressure-sensitive diaphragm is released by etching Si–handle layer by DRIE technique with utilizing a positive photoresist mask. Similarly, the device layer of SOI wafer is etched by DRIE to a depth of 40 μm to release resonant structures. A buffered hydrofluoric acid solution is used to release the resonant structure by undercutting the insulation layer in a controlled manner. For creating the metal connection, the Al–electrodes were sputtered on the front side of the bonded SOI-glass wafer by utilizing a shadow-mask technique as shown in the fig. 12 [117]. In fig. 13, A 1 μm thick PZT layer is etched by the

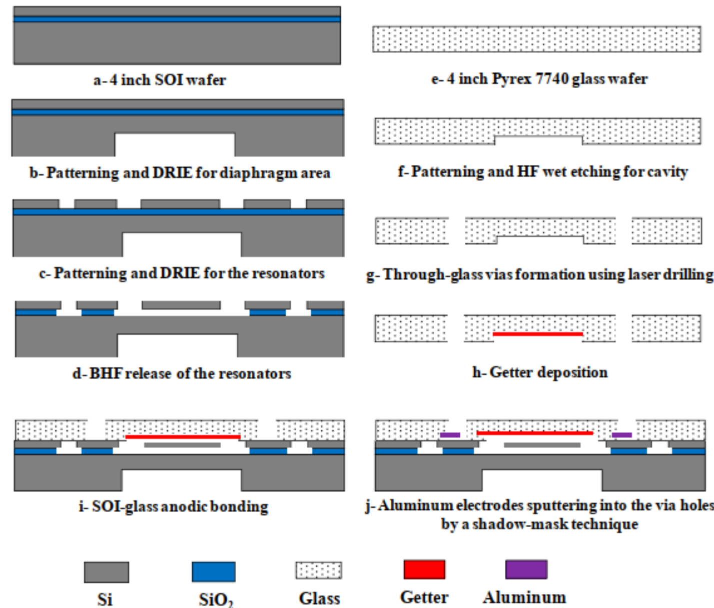

Figure 12: Various fabrication steps involved for the micro– resonant pressure sensor [117]. (Reprinted with permission from figure [117])

wet etching solution on a 0.5 μm thick BOX layer of SOI wafer followed by Au layer of 0.3 μm thick is deposited and patterned by using the lift-off process. The ICP etching technique is used to remove the PZT layer, Pt layer and Si–device layer. Finally DRIE and RIE techniques are used for the back side Si–etching and BOX layer etching respectively [118]. Fig. 14 shows SEM view of fabricated Si–MEMS Microflap resonator and Si–MEMS bridge resonator [119].

3.4. Etching

There are various parameters that affect the etching processes such as etch rate, uniformity, selectivity and directionality [120]. The speed of the etching should be in controllable manner but fast enough for production. Based on the directionality aspects etching is classified as isotropic etching and anisotropic etching. In the first case, the etching rate do not depend on direction i.e., uniform in all directions. Therefore a semi-circular shape profile is obtained under the mask whereas in case of anisotropic etching, the dissolution of the material takes place only in vertical direction and a

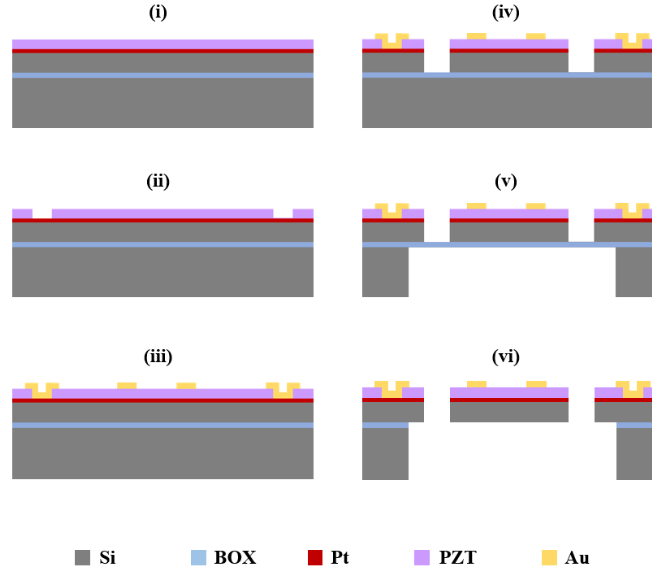

Figure 13: Process flow of Fabrication steps for TPoS resonant sensor: (i) A SOI wafer with application of Pt and PZT layers. (ii) Etching of PZT layer. (iii) Lift-off process for patterning of Au layer. (iv) The inductively coupled plasma etching process for PZT, Pt and silicon device layers. (v) DRIE technique for the back-side Si–etching. (vi) RIE technique for etching the Buried oxide layer [118] (Reproduced the figure with permission from [118])

straight walls profile is obtained [121]. Du et al. fabricated the BDETF resonator by using anisotropic wet etching technique with a 25 wt% Tetramethyl–ammonium hydroxide (TMAH) solution and the resonant layer is produced by chemical mechanical polishing (CMP) technique [122]. This shows that anisotropic etching is meant to etch faster in one particular direction i.e., Si111-crystal plane in contrast to Si 100 plane [123, 124]. Wet etching techniques with the help of various acids and bases solution combinations can be utilized for metal etch. TMAH, Potassium–hydroxide (KOH), ethylene–diamine pyrochatechol (EDP) are some of the important etchants available for Silicon [125]. Wet etching can be utilized for obtaining anisotropic directional etches on crystalline material. There are two approaches for etching silicon oxide (SiO2) using hydrofluoric acid (HF) vapor [126]. Several parameters have a direct impact on the etch rate silicon oxide such as wafer temperature, partial pressures of HF and catalysts. Li et al. investigated the presence of 300 nm gap in between resonator and electrode which improves

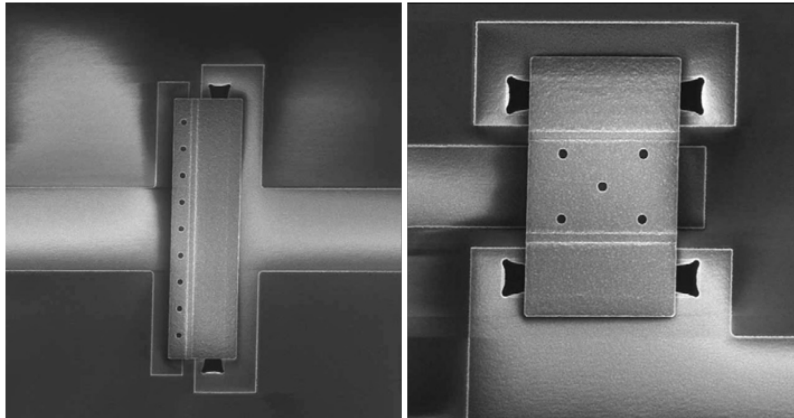

Figure 14: SEM view of fabricated Si–MEMS Microflap resonator (left) and Si–MEMS bridge resonator (right) [119] (Reprinted with permission from [119])

the electro–static coupling when a poly–Si etching is done before Metal etching in CMOS–MEMS resonant transducer [127] Doping of boron in silicon significantly reduces etch rate of KOH [128]. Tabrizian *et al*. described the fabrication of piezo–on–substrate and used isotropic wet etching technique for high etch selectivity of AlN over bottom–electrode and also provide a slopped–wall of AlN to ease consistent coverage during deposition of top metal [129].

Pakpum *et al*. [130] studied the condition for achieving etching of 90 deg vertical wall on Si100 substrate using 45% (wt. fraction) of NaOH and solution temperature of 40 °C. Several investigations on achieving a better etch characteristics were studied in the past. The etching rate of Si110-crystal plane with a solution of etchants at (20%wt) KOH and (15%wt) NH_2OH has shown four times increase in etching in contrast to only solution of (20%wt) KOH [131]. Dry etching technique involves both chemical and physical attacking on material. Directionality in etch can be obtained by using different mechanisms such as reactive–ion etching (RIE), high–pressure plasma etching and ion milling. RIE technique uses a chlorine (Cl) gas based low pressure plasma to remove deposited material on Si and GaAs wafers [132]. In RIE process, the EM field assists in the generation of the plasma under vacuum. This plasma breaks the feed gases into ions, which are accelerated towards the wafer and reacts with its surface. These ions after obtaining high grade energies can even de-notch the materials out of a wafer without a chemical reaction. With the increase in the gas flow in the chamber, there was a net

increase in etchant flux which in turn shows improved impinge action on the substrate thereby was helpful in enhancing the etch rate [133]. Arcamone *et al*. [134] fabricated a resonator using SOI wafer as substrate. The micro fabrication starts with n-type doping of the top device layer by diffusion followed by thermal activation of these impurities via O_2 and N_2 atmosphere. the next step involves the patterning of the sample after the resist coating via electron beam lithography. Kaajakari *et al*. further demonstrated a bulk acoustic resonator, which is fabricated on SOI wafer using deep reactive–ion etching (DRIE) indicating stability of approximately 1 ppm/year [135]. In addition to it, Abe *et al*. [136] proposed a fabrication technique for quartz-based resonator having a deep etched structure. These resonators are very sensitive to surface tempering so, in order to improve the resonators performance, the precise variation of surface shape below 1 μm is desirable for thin resonant device. The etch selectivity is very small for quartz and photoresist. Wood *et al*. [137] fabricated a MEMS resonator with a 150 mm Silicon-on-insulation substrate with 30 µm thick device layer. The resonator is patterned by using DRIE technique of 5 μm trenches in the device layer of 30 μm. Followed by the HF etching for BOX layer that release the resonator from the substrate. The author demonstrated the variation in the ratio of vibrating amplitude of two fabricated resonators by decreasing the mass of one of the resonators through Forced ion beam milling. The SEM view of the fabricated resonator is shown in the fig 15.

Liu *et al*. [138] reported the threefold enhancement in Q factor of thin film piezoelectric on silicon MEMS resonator based on a phononic crystal (PnC) reflector composite. Fig. 16 shows the proposed design for the resonator were presented on AlN on SOI substrate, with first step of deposition a layer of phosphosilicate glass followed by the annealing in the presence of Ar gas at 1050 °C so as to make the top layer of substrate as conductive. The second step, is the thermal oxidation and patterning of 200 nm thick SiO2 layer in between the electrode and the ground. Further a 500 nm thick AlN film was deposited on the substrate by the reactive sputtering, followed by the deposition of 1 μm thick Al and 2 μm thick Cr layer by electron beam evaporation techniques. DRIE process is used to etch the SiO_2 layer so as to release the support of beam structure and PnC structure. A layer of Polyimide is deposited as top layer to mask the device structure and followed by a sequence of RIE and DRIE, to etch the bottom layer of oxide for the first and second time respectively. The SiO_2 is then etched with hydrofluoric acid to remove SiO_2 layer so as to release the designed resonator structure.

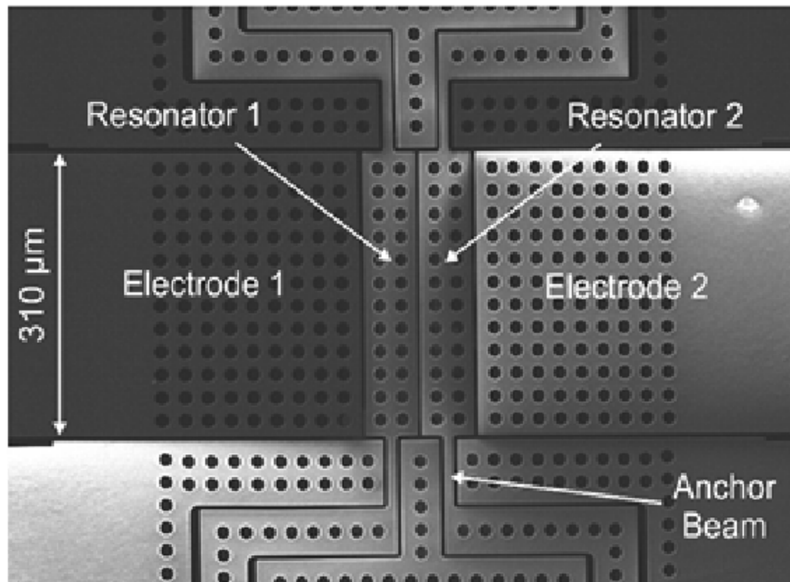

Figure 15: SEM view of micromachined coupled-resonator [137]. (Reprinted with permission from [137])

Chen *et al*. developed a resonant pressure sensor and demonstrated the limit of measurement of the sensor to be 1 MPa. The various fabrication steps involved in the micromachining of the resonator are shown in the fig. 17 [139].

Han et al. presented the use of wet etching technique with TMAH solution and a 500-nm thermal oxidation SiO2 mask. For creating bonding between resonator layer and diaphragm layer, Si–fusion bonding method is adopted and boron-doping piezo–resistors are fabricated using ion–implantation. For obtaining ohmic contact P-ion implantation is performed followed by the lift-off process to release Al metal contact. Then, DRIE process assists to release the overall 4.7 mm × 5.7 mm size structure of the resonant pressure sensor [140]. Blue et al. reported a novel design for the MEMS triple-beam resonator which is based on the temperature induced resonance frequency shift as shown in the figure 18 [141]. Zhang et al. designed an electrostatically actuated comb drive pressure sensor on silicon-on-insulation substrate. Figure 19 shows the following (a) Image of a patterned SOI wafer after anodic–bonding between the SOI and the glass. (b) view of fabricated resonator with comb-drive electrodes. (c) proto–type view of resonator with a dimension of 7 × 7 mm2. (d) resonant sensor mounted on top of a covar–header [142].

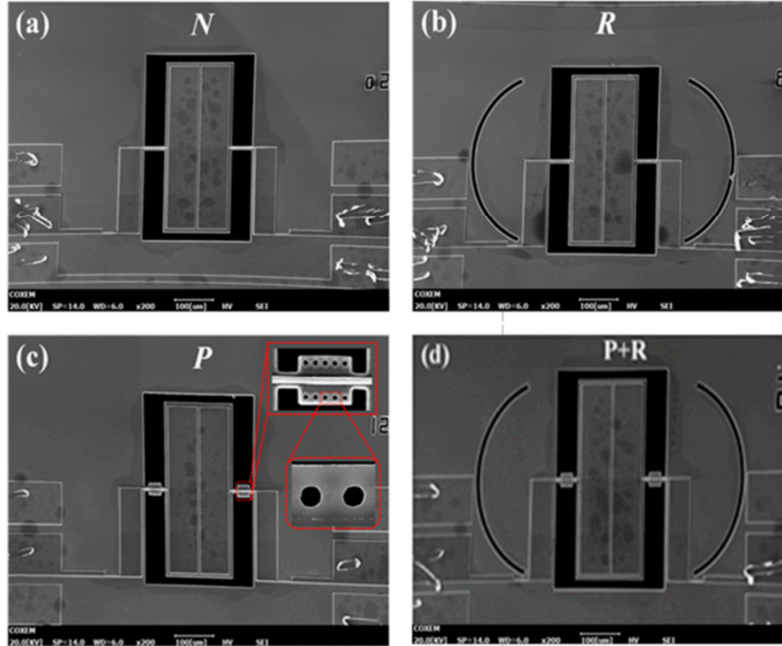

Figure 16: The TPoS resonator as seen from a SEM. (a) Traditional structure; (b) quarter–wavelength reflector structure; (c) phononic crystal on the supporting tether (d) phononic crystal–Reflector Composite microstructure [138]. (Reprinted with permission from [138])

Kuo *et al*. [143]integrated a multiple sensor on a single innovative System–on–chip design resonator structure. The fabrication of the proposed MEMS resonator is performed using UMC 0.18 μm 1–poly 6 metal CMOS/ MEMS's process followed by anisotropic and isotropic etching technique to released MEMS structure. The fabrication of MEMS resonator is performed after removal of the passivation layer above the MEMS_MASK area via dry etching to define the CMOS circuitry processing. Fig. 20 shows, (a) METAL7 layers preserves the region for the microstructure after determining dry etching. (b) The application of photoresist followed by the anisotropic DRIE etching and (c) the release of resonator microstructure after isotropic Si etching. Lin *et al*. [144] present the SoC design for resonator-based thermometer operating at -40 °C to 120 °C having a sensitivity of -5.7Hz/°C with a much lower power utilization of readout circuitry of 190.4 μW. Tseng *et al*. [145] proposed a SoC design for CMOS/MEMS resonator the DC/DC converter. The oscillation frequency measured is up to 35.2 kHz with a 30V DC voltage.

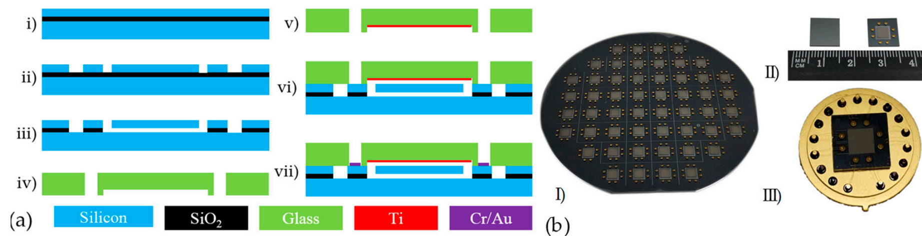

Figure 17: (a) The fabrication processes (i) Cleaning of SOI wafer; (ii) leaving window for the sensing elements; (iii) Releasing of resonators structure; (iv) Forming the through-glass via and cavity in glass wafer; (v) Sputtering technique used for Ti as getter; (vi) Anodic–bonding; (vii) formation of Cr/Au metal contact. (b) The micro–fabrication results: (I) Wafer after metal contact; (II) Resonant sensor chips after dicing; (III) Packaging step [139] (Reprinted with permission from reference [139]).

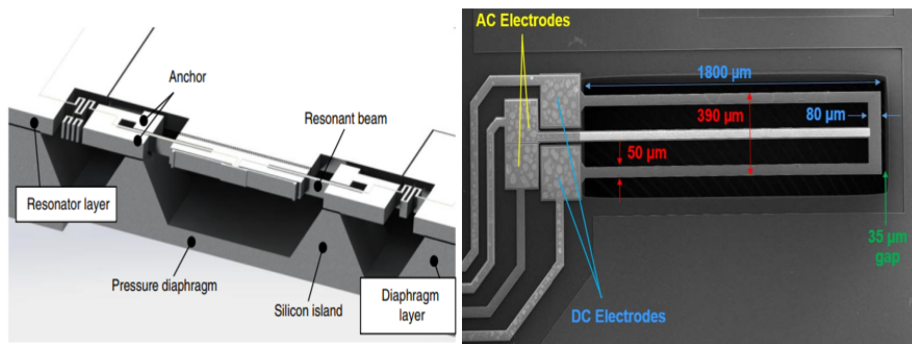

Figure 18: Cross–section image of the resonant pressure sensor (left) and SEM view of MEMS Si-triple beam resonant sensor (right) [141] (Reprinted with permission from [141]

Garg *et al*. [146] proposed a fabrication approach for Si 3D micro and nano-structure for the precise control and selective etching of an ion implanted pattern via focused ion beam (FIB) technique. The developed technique shows dedicated approach for the fabrication of 3D micro and nano structures with high aspect ratio architecture such as nano-mesh, nano-pyramids, and nano-wires. The techniques such as nano-lithography, are restricted to the patterning of resist materials, Focused-ion beam allows patterns to be created in practically any material. Regrettably, the procedure is sluggish. The material removal rate for a 30 keV gallium ion in most materials is about 1–10 atoms/incident ion, in contrast to a machining rate of 0.1–1 μm^3/nC of incident ions [147].

Xiong *et al*. [148] fabricated an oscillating probe of atomic force micro-

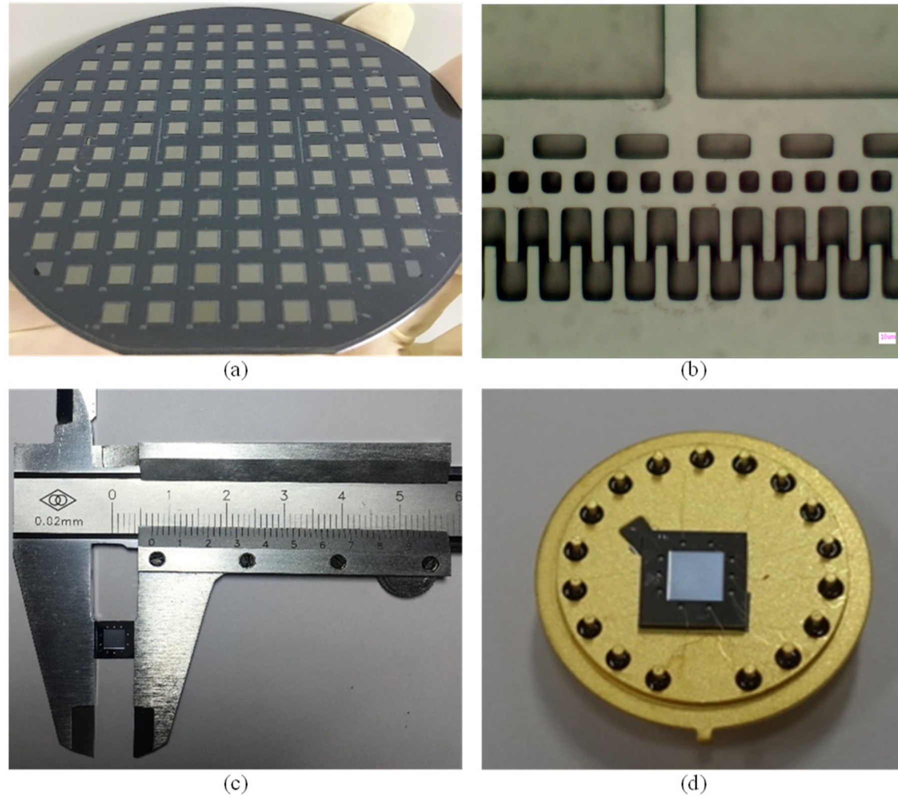

Figure 19: (a) Image of a patterned SOI wafer after anodic–bonding between the SOI and the glass. (b) Micro–scale detailed view of fabricated resonator with comb-drive electrodes. (c) Image of a proto–type sensor with a dimension of 7 × 7 mm2. (d) Image of a fabricated resonant sensor mounted on top of a covar–header [142] (Reprinted with permission [142])

scope (AFM) by utilizing electrostatic excitation and piezoresistive detection. The fabrication of micro-resonator starts with SOI wafer. The phosphorus is implanted to 200 nm deep to make the piezo resistors of 5× 10 17 atoms/cm^{-3} for about 21 nm below the surface followed by the thermal deposition of metallic pads consisting of Cr, Pt and Au materials. The resonator structures are patterned on the top layer of SOI by using Deep reactive ion etching (DRIE) technique. The substrate is then coated with the thick resist followed by the DRIE technique to release the handle layer. The BOX (buried oxide) layer is then etched by using BHF for 30 min to release the final micro ring-resonator via CO_2 drying process.

Wang *et al*. [149] demonstrated a fabrication steps for the wavelength

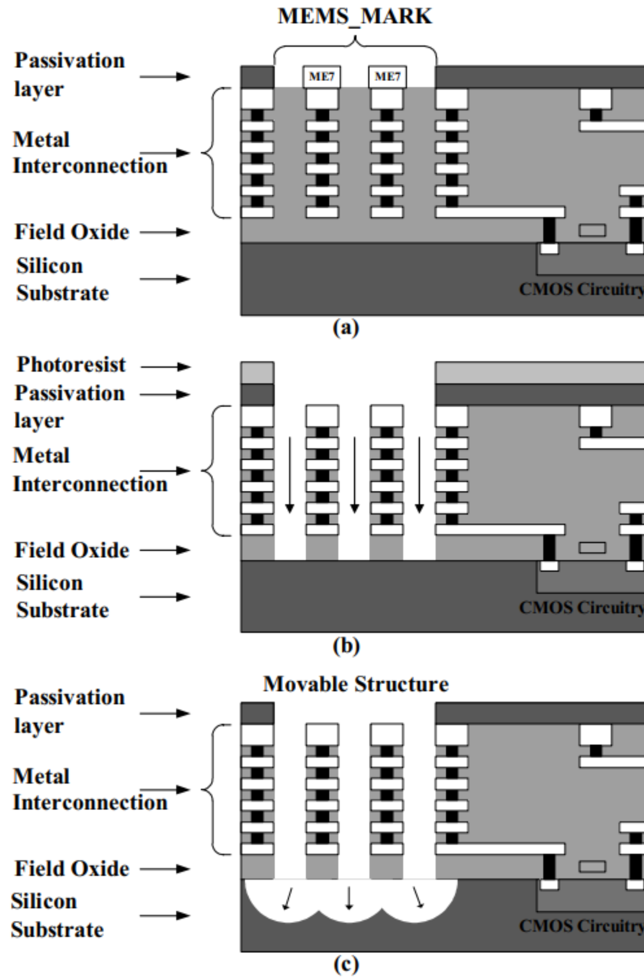

Figure 20: Cross-sectional image of ASIC/MEMS process [143] (Reprinted with permission from [143])

sized micro-disk type resonator in Silicon carbide thin-film-on-insulation (SiCOI). Fig. 24 shows the micro-manufacturing of the micro-disk resonator initiated with a 300 nm thick methyl methacrylate (MMA) layer and poly methyl methacrylate layer (PMMA) were spin coated onto the SiCOI wafer. The micro-disk patterned are structured using an electron beam lithography. After placing the wafer having solution of methyl isobutyl ketone and isopropyl alcohol is in a ratio of 3:1 for 45 s, a thick film of Cr has been deposited. The micro-disk structures are then released by dry etching via inductively

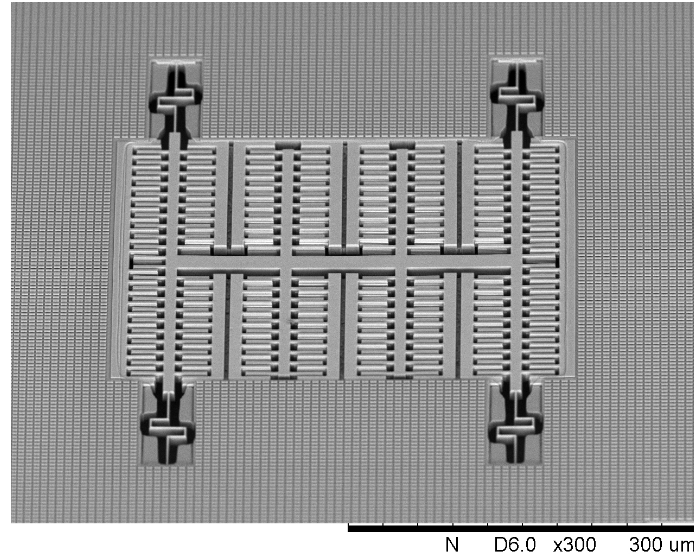

Figure 21: Magnified–SEM view of the resonator [144] (Reprinted with permission from [144])

coupled plasma reactive ion etching (ICP-RIE). Followed by the removal of BOX layer via HF acid to release a supporting pedestal.

SiC shows a high chemical stability, which makes the materials to be used in the harsh environment and deals with the biocompatibility issues therefore, favors epitaxial growth. The large semiconductor band gap offers high hardness, young's modulus and bulk modulus. The presence of dielectric (AlN) and a wide band gap SiC, shows high crystallo - chemical fully consistent thermal expansion coefficients [150]. SiC also is suitable as the functional layer due it its high stiffness. The piezoelectric stress coefficient of silicon carbide is smaller than other elements present in the group-III-nitride. Brueckner *et al*. demonstrated a SiC as substrate for the epitaxial heterostructures growth of GaN [151]. Jun *et al*. [152] fabricated an NEMS resonator using a combination of techniques such as electron beam lithography and a reactive ion etching. A thin epitaxial film of SiC is been deposited on the Si wafer using atmospheric pressure chemical vapor deposition (APCVD) technique. On the surface of SiC patterns are created using e-beam lithography followed by metal contact deposition and lifting-off process of aluminum. The device structure is released via a reactive ion etching using CF4 and O_2 in the ratio of 9:1, which resulted in the etching of SiC anisotropically for the release of

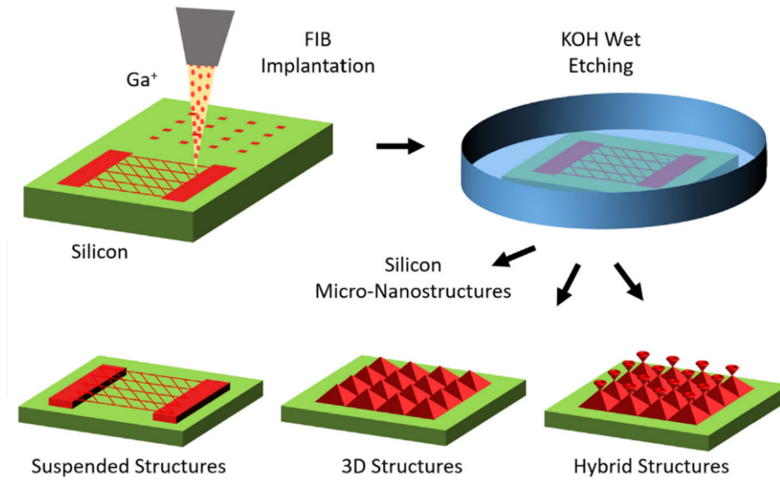

Figure 22: The schematic diagram of 3D micro-nanostructures with an ion beam via bulk Si structuration. [146] (Reprinted with permission from [146])

beam structure. On the application of direct current, these beams show a frequency tunning 10%. Magyar *et al.* [153] presented a fabrication technique for the micromanufacturing of micro-disk resonator using SiC as substrate. The fabrication initiates with p-type epitaxial SiC film on a n-type SiC substrate. The higher doping level of the substrate provides a low-resistance path for the structure's local cathode, allowing for efficient photo-generated electron extraction. The p-type SiC layer was aluminum doped and a 100 nm thick Ni layer is deposited on the n-type side to obtain the electrical contact for photoelectrochemical etching. The next step in fabrication is the annealing of the sample at 900 °C for 1 hr for the creation of the ohmic contact with silicon carbide. The micro-disk pattern on the epilayer is transferred to the SiC by using a technique known as plasma reactive ion etching in the presence of SF6 and O_2 at a pressure of 5 mT. The etching is performed for 5 min for a total depth of 1200nm. The selectively etch the n-type material and undercut micro-disk, the sample is placed in 0.2 M KOH solution for 15 hr with a bias voltage of 0.2V.

3.5. Challenges in the fabrication

The diversified field of Micro-electromechanical systems application has created a huge challenge for its packaging in contrast to IC packaging; as these micro systems respond to various stimuli such as thermal, chemical,

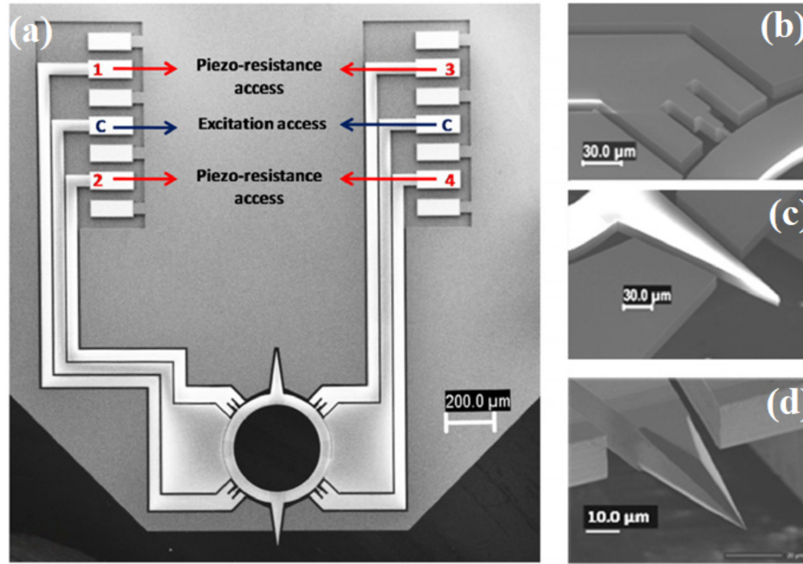

Figure 23: Scanning electron microscope view. (a) Structural overview. At the ring's quasi-nodal points, the anchors are placed. Each anchor has its own track that connects it to the metal pads. (b) The anchor's shape is intended to reduce the ring's frequency shift effect. (c) A Close-look at 200-μm tip. (d) FIB etching sharpened the tip [148]. (Reprinted with permission from [148].)

physical and many more. In the overall MEMS development process, packaging consumes both time and money. An effective package protects the micro device and allows it to perform with less attenuation in given surrounding [154]. Fabricating a precise high frequency resonator is challenging due to their small scale features, which are greatly influenced by sub-micron size variations [109]. The micro-devices that do not interact with the environment, those devices after fabrication process can be fully-encapsulated. Generally, there are two-level packaging used for MEMS resonator, namely wafer-level and conventional packaging. A resonator is to be kept in the cavity so as to protect it against the mechanical movement. The stability of the resonance frequency of the resonator decreases when the resonator is not hermetically encapsulated [155]. Wu *et al.* [156] deigned a wafer level packaging solution for the MEMS resonator devices. The cap wafer ensures a vacuum chamber to secure the moving components of resonator structure and to improve the resonator sensing performance along with the redistributing the electrical feed through via Si bumps. There are various constrains in the performance of MEMS/NEMS resonator, one of which is due to the

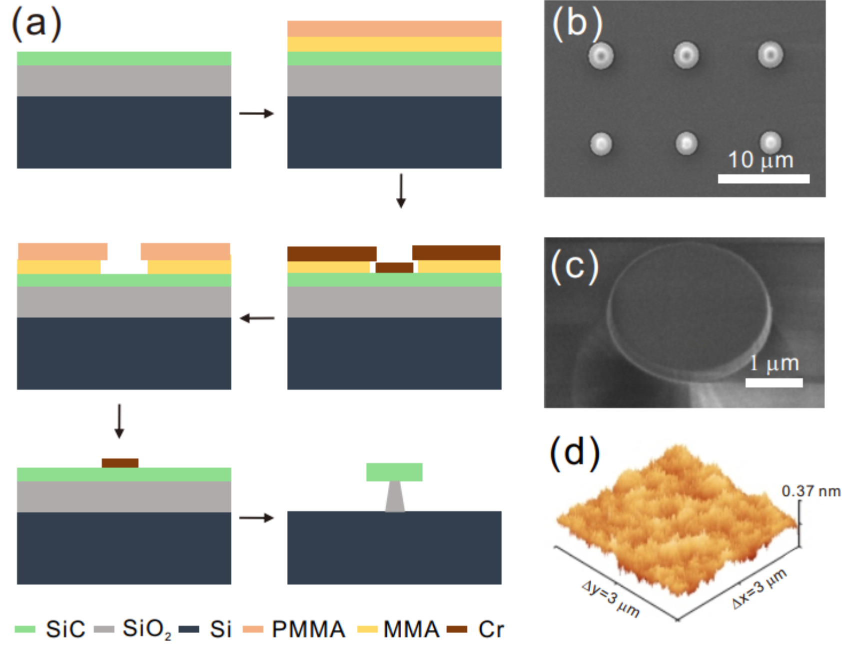

Figure 24: (a) Fabrication process flow of the wavelength-sized micro-disk resonators in 4H-SiCOI. (b) SEM image of the fabricated micro-disk array with different radius. (c) A zoomed-in SEM image of a single micro-disk resonator featuring with a radius of 1.5 mm and thickness of 160 nm. (d) 3D atomic force microscopy scan of the top surface of SiCOI [149] (Reprinted with permission from [149]).

dissipation mechanisms. Rodriguez *et al*. [157] demonstrated the variation in the measurement of the Q factor of Si MEMS resonator with the change in design, dimension and anchor for the detection via Akhiezer dissipation.

Table 3: Various packaging parameters based on experiment [158]

Packaging parameter	**Challenges**
Stiction	Release of devices
Dicing	Risks of contamination
Die–handing	Device's failure
Stresses	Degradation of performances
Testing	Failure of device after final assembly step

Structure adhesions to the system and poor tribological performance cause the introduction of failure to MEMS resonator, which can be improved

via chemical and tribological modification of the surface, thin and dual- film coating etc. Testing of the MEMS resonator plays a significant part in improving its performance and consistency. However, device testing devours up to 35% of overall fabrication cost [159].Therefore MEMS resonator fabrication requires a dedicated efforts and huge research knowledge. Some of the failures that can occur in MEMS resonator are due to sticking, severe ecological state, static overload, fatigue and so on. Xie *et al*. [160] studied the fabrication issues such as short circuit problem of MEMS sensors, which occur due to presence of (a) Si residue along the terminal-trench and (b) metal-stringers along trench surface. Failures due to stiction in resonator are caused by residual-stresses, electrical-static forces and van–der walls forces. However, these problems can be rectified by (a) preparation of hydrophobic surface, (b) reduction in contact area and (c) minimizing adhesion [161]. The performance of MEMS resonator is also depending on the effect of friction and wear. The alloy of Ni-P containing 15% Phosphorous is showing better mechanical properties than pure Ni. Therefore, metallic alloys is extensively used for the electroforming of the LIGA parts [162].

Table 4: Various parameter of failure for MEMS device [161]

Possible modes of failure	**Reasons**
Metallic contaminations	Various steps in fabrication, environmental response
Mechanical fracture	Fatigue cracking, Impacts, Friction and Overloading
Creep	Thermal and applied stresses
Wear	Corrosion, adhesion, surface fatigue
Electrical short circuit	Ohmic contact, contamination, oxidation

4. Recent progress on Si-MEMS resonant sensors

Kourani *et al*. demonstrated the design of AIN–on–silicon MEMS oscillator for the system of frequency compensation in cellular handsets application with a frequency stability of ±0.5 ppm over the temperature–range of -40 to 85 °C [163]. Amiri et al. presents a highly sensitive temperature sensor based on Si–oxynitride waveguide micro–ring resonator using broad–band input spectrum with a diameters of 1.27 mm and investigated the increase of Q factor in range of 15000–to–22000 w.r.t temperature, so as to function at different and longer wavelength–band [164]. Okabe *et al*. has proposed a Si–based antenna by using a LC resonator, measures the resonant frequency

of fabricated antenna to be 465 MHz with a gain of -35.75 dBi due to its smaller size [165]. Zhao *et al.* presented a MEMS sensing chip with a micro–cantilever to monitor different gas pressures, under resonance frequency shift conditions. The maximum deviation of the resonance frequency was observed to be 59 ppm over the full pressure and at the temperature–range of 26-55 °C [166]. Charkhabi *et al.* compared the three different fabrication techniques to produce flexible–LC resonant sensor via screen–printed pastes, wound metal–wires and etched Cu-coated polyamide and analyze the resonance frequency and peak–to–peak amplitude of scattering parameters [167]. Dezest *et al.* experimentally investigated the transduction efficiency by implementing 150 nm thick piezoelectric layer to the NEMS resonator and obtain a Q–factor values (Q = 900 in a vacuum and Q = 130 in air) at room temperature for resonant responses in the MHz–range [168]. Su *et al.* presented the design and fabrications results of a pressure modulated resonant sensor, to measure pressure in range of 40kPa to 120kPa, with a maximum sensitivity of 73.125 kHz/kPa, corresponding to a temperature range of 24 °C to 800 °C [169].

Belsito *et al.* reported a micro–fabrication of resonant strain–sensor on SOI by LPCVD process. The sensors performances on structure materials are obtained for both positive and negative strain regimes, resulting in the resolution limit of 150 pϵ and sensitivity of 16 Hz/$\mu\epsilon$ over a bandwidth ranging from 1.5 to 50 Hz [170]. Cimielli *et al.* investigated different SOI micro–cavities planar geometries on a ring¬–shape, disk–shape and hybrid–configurations for biochemical sensing, and propose a resonator devices having Q–factor value as 1.73×105, sensitivity of 120 nm/RIU and detection limit of 10-6 RIU for sensor [171]. Bakula *et al.* investigated the use of a quartz-based MEMS tuning fork resonator for wireless electrical–power reception unit as an alternative of magnetic field, for implantable devices with an acoustic feed–back unit. On measurement Q factor yields the values (Q = 7000 for encapsulated , Q = 8400 for decapsulated and Q = 1700 for magnet–loaded tuning fork) [172].

Fang *et al.* demonstrated the experiment evaluation of a Si–resonant accelerometer, showing an increase in scale factor value to 361 Hz/g with a long term stability of 1.77 μg in a time frame of 30–days under ±0.01 °C controlled temperature variation [173]. Le *et al.* proposed a micro–cantilever based resonant humidity sensor excited by inter–digital transducer technique using AIN/Si layer structure. On its comparison with normal electrode, an increased in sensitivity is observed from 9.67 –to– 84.41 Hz/%RH with a

smaller temperature–coefficient of frequency as -23.6 ppm/°C [174]. Qiangxian *et al*. experimentally investigated the use of Si cantilever for high order resonant mode AFM. The canning speed and high order resonance is a characteristic of Q factor, amplitude and the mode–shape of the Si cantilever, having the resolution of first order and second order resonance to be as 0.83 nm, 0.42 nm respectively [175]. Ghosh *et al*. presented a fabrication of magnetometer based WE mode thin film–piezoelectric–on –Si resonator showing the resonance frequency as 18 MHz and Q factor value (Q = 1500) and sensitivity as 63.27 mV/T under room temperature [176].

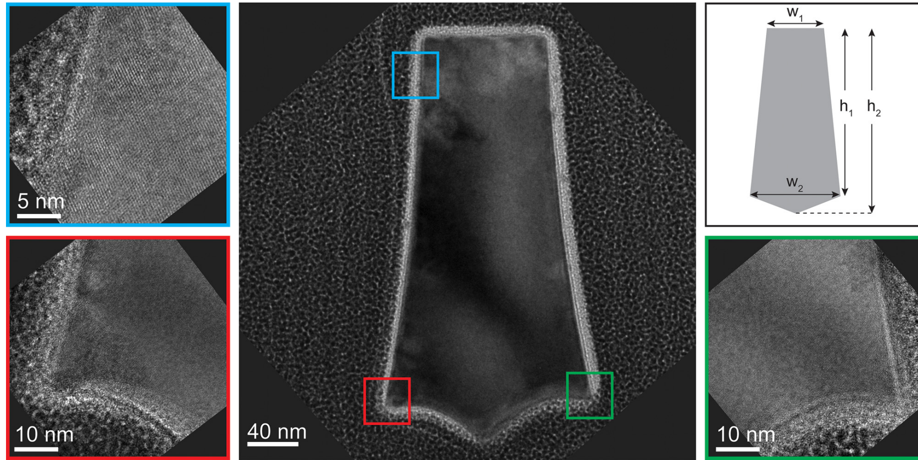

Figure 25: The trapezoidal Si NW cross-section as seen via high-resolution TEM photograph. Close-up views from various zones of the Si NW are depicted in the insets [177]. (Reprinted with permission from [177].)

Sugano *et al*. fabricated a micro–resonator with Si covered gold nano–rods for the detection of near–infrared laser wavelength shifting, with resolution and maximum resonant frequency shift of 0.37 pm and 69 Hz/nm respectively [178]. Patocka *et al*. presented a piezoelectrical based Si–micro cantilever for detection of small sized particles having dielectric properties in liquid medium, showing the detection limit and mass responsively in the range of 3.5 ng and 1 Hz/ng respectively [179]. Mahdavi et al. proposed a novel dew point meters having thin film piezoelectric on Si–resonator, whose long term accuracy and reliability is measured by conducting 35,000 uninterrupted cycles of measurements and investigated the dew–point temperature to be as low as -41 °C [180]. Mohammadi et al. proposed a phononic–crystal resonant structure which is fabricated by etching a honeycomb array of air–holes

silicon slab. This fabricated resonator get excited at 120 MHz and 129 MHz, corresponding to a flexural mode and extensional mode respectively [181].

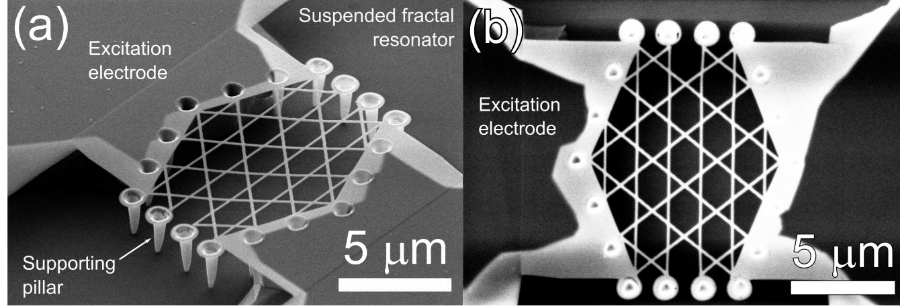

Figure 26: Images of the fractal nanostructure taken with a scanning electron microscope (SEM): (a) SEM micrograph of the suspended fractal resonator tilted 45 degrees. (b) Top-view SEM micrograph of the suspended structure [182]. (Reprinted with permission from [182]).

Phillippe *et al.* [183] presented a co-integration of NEMS-CMOS oscillator having 0.35 μm circuit on a Silicon-on-insulation substrate. The oscillator works at a bias voltage of 24 V and 7.8 MHz. Li *et al.* [184] demonstrated a nano-scale force and pressure sensor integrated with triple nano ring (TNR) resonator having resonant peak with Q factor of 1602 and 1737 for Si and Si/SiO_2 diaphragm respectively. The NEMS resonator has an added advantage as it becomes insensitive to the vibration due to their lower mass and therefore are suitable for the stable frequency sources [185] . Rinaldi *et al.* [186] demonstrated the ultra–thin piezoelectric resonator and filters for the super high frequency (SHF) range for wireless communication purpose. Esfahani *et al.* [187] presents a fabrication of piezoresistive based silicon nanowires resonator for obtaining resonance behavior of NEMS resonator with frequencies of 100 MHz showing a Lorentzian non-linear behaviour with Allain deviation of 3-8 ppm. The various steps involve in the fabrication of the Si NW on SOI wafer are summarized as (a) e–beam patterning of silicon nanowire, (b) bilayer patterning lift-off mask, (c) metallic coating by thermal-evaporation followed by lift-off (d) Si etching (e) low temperature oxide coating via LPCVD (f) oxide etching (g) MEMS patterning (f) deep etching of Silicon via bosch process (i) hydrofluoric acid releases the NW [177] as shown in the fig. 25. Vassil *et al.* [182] fabricated the resonator on SOI wafer with 2 μm having device layer. The resonator structure contains seven–star polygons arrange in a fractal structure. The wafer is then

diced into 1 × 1 cm^2 and are directly patterned by focused ion beam (FIB) implantation of Ga+ with energy, beam current and dose as 30 Kev, 10 pA and 1 × 106 per cm^2 respectively. The SEM image of the fabricated NEMS resonator is shown in the fig. 26.

Table 5: Recent review papers based on MEMS Resonator.

Sr. no	Authors	Paper title	Main Objective	Year	Ref.
i.	A. Uranga, J. Verd, N. Barniol	CMOS–MEMS resonators: From devices to applications	This review paper shows CMOS–MEMS resonator integration, for the application as oscillator circuits in sensory system.	2014	[188]
ii.	Reza Abdolvand , Behraad Bahreyni , Joshua E. -Y. Lee and Frederic Nabki	Micro machined Resonators: A Review	This paper describes the model and properties of generic micro–resonator along with briefly discussing the application in the last three decades.	2016	[189]
iii.	Chun Zhao Mohammad H. Montaseri Graham S. Wood Suan Hui Pu Ashwin A. Seshia Michael Kraft	A Review on MEMS Coupled Resonators for Sensing Applications Utilizing Mode Localization	In this paper a mode–localized MEMS coupled resonator sensor is use for the study, and its effects are discussed for measuring sensitivity.	2016	[190]

iv.	Olebogeng Bone Kobe, Joseph Chuma, Rodrigo Jamisola Jr, Matthews Chose	A review on quality factor enhanced on-chip microwave planar resonators	In this paper a detailed study on enhancing the Q–factor and related technique is studied in depth for a microwave on chip resonator.	2017	[191]
v.	Liting Gai, Jin Li, Yong Zhao	Preparation and application of microfiber resonant ring sensors: A review	This paper summaries the various micro–manufacturing technique and application of different type of micro–fiber resonator ring.	2017	[192]
vi.	Y. Tsaturyan, A. Barg, E. S. Polzik and A. Schliesser	Ultra-coherent nanomechanical resonators via soft clamping and dissipation dilution	This paper reviews the novel methods used for determining resonators nanomechanical modes for spatial confinement and reduction in material's intrinsic dissipation.	2017	[193]

vii.	M. Tlili, F. Deshours, G. Alquié, H. Kokabi, S. Hardinata, F. Koskas	Microwave Resonant Sensor for Non-invasive Characterization of Biological Tissues	This paper investigated the use of microwave ring resonator for monitoring various vital signs such as temperature, heartbeat etc. and characterization of biological–tissues.	2018	[194]
viii.	Yuting Wang, Yao Pan, Tianliang Qu, Yonglei Jia, Kaiyong Yang and Hui Luo	Decreasing Frequency Splits of Hemispherical Resonators by Chemical Etching	This paper investigated the use of chemical etching technique to decrease the frequency split below 0.5 Hz of hemispherical resonator.	2018	[195]
ix.	Saad Ilyas, Mohammad I. Younisb.	Resonator-based M/NEMS logic devices: Review of recent advances	In this paper, recent progress and challenges in the frequency tuning of resonator-based MEMS/NEMS logic devices is discussed.	2019	[196]

x.	Maria C. Cardenosa-Rubio, Heather M. Robison and Ryan C. Bailey	Recent advances in environmental and clinical analysis using micro ring resonator – based sensors	This paper summarizes micro ring resonator for the application of clinical detection and environmental issues. Also thoroughly describe the sensing principle and fabrication technique based on reviewing various articles.	2019	[197]
xi.	A.Z. Hajjaj, N. Jaber, S. Ilyas, F.K. Alfosail, M.I. Younis	Linear and nonlinear dynamics of micro and nano-resonators: Review of recent advances	This paper overviews the linear, non–linear and the dynamic behavior of various MEMS and NEMS resonators.	2019	[198]
xii.	Simone Berneschi, Francesca Bettazzi, Ambra Giannetti, Francesco Baldini, Gualtiero Nunzi Conti, Stefano Pelli, Ilaria Palchetti	Optical whispering gallery mode resonators for label-free detection of water contaminants	This paper reviews the use of Whispering Gallery Mode (WGM) resonator platforms for high performance monitoring of environmental contaminants.	2020	[199]

xiii.	Cheng Tu, Joshua E.-Y. Lee and Xiao-Sheng Zhang	Dissipation analysis Methods and Q-Enhancement Strategies in piezoelectric MEMS Laterally Vibrating Resonators: A Review	In this paper, a comprehensive analysis of dissipation method and Q-factor enhancement strategies are discussed for piezoelectric MEMS vibrating resonator.	2020	[200]
xiv.	Gayathri Pillai, sheng shian li	Piezoelectric MEMS resonator: A review	In this paper, study is focused on the use of various thin film piezoelectric material with CMOS integrated microfabrication platform for resonator.	2020	[201]
xv.	The present review work summarizes the microfabrication aspects associated with MEMS and NEMS. This article also provides a gist on recent progress and fabrication challenges on Si based resonant sensors.				

5. Conclusion

The popularity of MEMS resonator has gained interest worldwide with the involvement of modern miniaturization technologies. MEMS resonator with miniature level dimensions, lower power consumption and low fabrication cost are opening its way for fabrication with new materials. In this review article, attempt has been made to highlight the state-of-the-art reviews on the work performed on Si-MEMS/NEMS resonant sensor and the variability in concepts and techniques that have been sought over the last two decades. Although the fabrication aspects of single-crystal Si and poly-Si processing dominated the literature, but this review work has demonstrated the wide range of microfabrication techniques used for Si based MEMS/NEMS devices that reflect the field's divergence today. Gist of the work associated

with piezoelectric films, bulk-materials and also micro-manufacturing technology in CMOS fabrication has been provided with this work. Drop in the testing charge, which is unswervingly related to the complexity in the device and the performance investigation of MEMS resonant devices has opened the commercial prospects for such devices. The scientific progression has invigorated researchers of this field to further reduce the devices to nanometers levels, such devices are called NEMS (Nano electro-mechanical systems) which has great possibilities to substitute MEMS devices due to its efficient integrities and enhanced functionalities in future.

Acknowledgements

Corresponding author would like to acknowledge the affiliating institute (IIT Jodhpur) to provide the research seed grant (I/SEED/AKG/20190022) and Start Research Grant (SRG/2020/001895) provided by Science and Engineering Research Board, Department of Science and Technology, India.

Conflicts of Interest

The authors declare no conflict of interest. The funders had no role in the design of the study; in the collection, analyses, or interpretation of data; in the writing of the manuscript, or in the decision to publish the results.

References

[1] Nadim Maluf. An introduction to microelectromechanical systems ngineering, 2002.

[2] Krishnakumar Sundaresan, Gavin K. Ho, Siavash Pourkamali, and Farrokh Ayazi. A low phase noise 100mhz silicon baw reference oscillator. In *IEEE Custom Integrated Circuits Conference 2006*, pages 841–844, 2006.

[3] Yu-Wei Lin, Seungbae Lee, Sheng-Shian Li, Yuan Xie, Zeying Ren, and C.T.-C. Nguyen. Series-resonant vhf micromechanical resonator reference oscillators. *IEEE Journal of Solid-State Circuits*, 39(12):2477–2491, 2004.

[4] Mr Viral Patel. A new emerging technology: Mems.

[5] Wan-thai Hsu. Vibrating rf mems for timing and frequency references. In *2006 IEEE MTT-S International Microwave Symposium Digest*, pages 672–675, 2006.

[6] Exchange M. What is mems technology? `https://www.mems-exchange.org/MEMS/what-is.html`, 2014.

[7] Ying Jian Chen. Advantages of mems and its distinct new applications. In *Metallurgy Technology and Materials II*, volume 813 of *Advanced Materials Research*, pages 205–209. Trans Tech Publications Ltd, 12 2013.

[8] Rabiul Al Mahmud, Md. Omar Faruque, and Rakibul Hasan Sagor. A highly sensitive plasmonic refractive index sensor based on triangular resonator. *Optics Communications*, 483:126634, 2021.

[9] Mohammad Islam, Ran Wei, Jaesung Lee, Yong Xie, Soumyajit Mandal, and Philip Feng. A temperature-compensated single-crystal silicon-on-insulator (soi) mems oscillator with a cmos amplifier chip. *Micromachines*, 9:559, 10 2018.

[10] Mohammad Danaie and A. Shahzadi. Design of a high-resolution metal–insulator–metal plasmonic refractive index sensor based on a ring-shaped si resonator. *Plasmonics*, pages 1–13, 2019.

[11] Louizos-Alexandros Louizos, Panagiotis G. Athanasopoulos, and Kevin Varty. Microelectromechanical systems and nanotechnology: A platform for the next stent technological era. *Vascular and Endovascular Surgery*, 46(8):605–609, 2012.

[12] Intel. The story of the intel® 4004. `http://www.intel.com/content/www/us/en/history/museum-story-of-intel-4004.html`, 2013.

[13] K.E. Petersen. Silicon as a mechanical material. *Proceedings of the IEEE*, 70(5):420–457, 1982.

[14] Guide P. History of mems. 23:1–10., 1990.

[15] PCMag. Definition of mems. `https://www.pcmag.com/encyclopedia/term/mems`, 2020.

[16] Rajeev Singh, Rishi Kant, Sushant Singh, Suresh Ellappan, Ankur Gupta, and Shantanu Bhattacharya. A novel helical micro-valve for embedded micro-fluidic applications. *Microfluidics and Nanofluidics*, 19, 07 2015.

[17] Akshay Atwe, Ankur Gupta, Rishi Kant, Mainak Das, Ishan Sharma, and Shantanu Bhattacharya. A novel microfluidic switch for ph control using chitosan based hydrogels. *Microsyst. Technol.*, 20(7):1373–1381, July 2014.

[18] Jumril Yunas, Budi Mulyanti, Ida Hamidah, Muzalifah Mohd Said, Roer Eka Pawinanto, Wan Amar Fikri Wan Ali, Ayub Subandi, Azrul Azlan Hamzah, Rhonira Latif, and Burhanuddin Yeop Majlis. Polymer-based mems electromagnetic actuator for biomedical application: A review. *Polymers*, 12(5), 2020.

[19] H. C. Nathanson, W. E. Newell, R. A. Wickstrom, and J. R. Davis. The resonant gate transistor. *IEEE Transactions on Electron Devices*, 14(3):117–133, March 1967.

[20] E.W. Becker, W. Ehrfeld, P. Hagmann, A. Maner, and D. Münchmeyer. Fabrication of microstructures with high aspect ratios and great structural heights by synchrotron radiation lithography, galvanoforming, and plastic moulding (liga process). *Microelectronic Engineering*, 4(1):35–56, 1986.

[21] Kevin A. Shaw, Z.Lisa Zhang, and Noel C. MacDonald. Scream i: A single mask, single-crystal silicon, reactive ion etching process for microelectromechanical structures. *Sensors and Actuators A: Physical*, 40(1):63–70, 1994.

[22] M. Mishra, V. Dubey, P. Mishra, and Isharat Khan. Mems technology: A review. 2019.

[23] Liudi Jiang and Rebecca Cheung. A review of silicon carbide development in mems applications. *International Journal of Computational Materials Science and Surface Engineering*, 2(3-4):227–242, 2009.

[24] Robert Osiander, J. Champion, Margaret Darrin, D. Douglas, T. Swanson, J. Allen, and E. Wyckoff. Mems shutters for spacecraft thermal control. 09 2002.

[25] Xinyu Liu, Martin Mwangi, XiuJun Li, Michael O'Brien, and George M. hitesides. Paper-based piezoresistive mems sensors. *Lab Chip*, 11:2189–2196, 2011.

[26] Tomasz Blachowicz and Andrea Ehrmann. 3d printed mems technology—recent developments and applications. *Micromachines*, 11(4), 2020.

[27] H Rashidzadeh, PS Kasargod, Tareq Muhammad Supon, Rashid Rashidzadeh, and Majid Ahmadi. Energy harvesting for iot sensors utilizing mems technology. In *2016 IEEE Canadian Conference on Electrical and Computer Engineering (CCECE)*, pages 1–4. IEEE, 2016.

[28] Jennifer A Rice and BF Spencer Jr. Structural health monitoring sensor development for the imote2 platform. In *Sensors and Smart Structures Technologies for Civil, Mechanical, and Aerospace Systems 2008*, volume 6932, page 693234. International Society for Optics and Photonics, 2008.

[29] Sudarsana Jena and Ankur Gupta. *Embedded Sensors for Health Monitoring of an Aircraft*, pages 77–91. 01 2019.

[30] Different types of wireless communication protocols in iot. `https://iotdesignpro.com/articles/different-types-of-wireless-communication-protocols-for-iot`, 2020.

[31] Tyronese Jackson, Katrina Mansfield, Mohamed Saafi, Tommy Colman, and Peter Romine. Measuring soil temperature and moisture using wireless mems sensors. *Measurement*, 41(4):381–390, 2008.

[32] Sudarsana Jena, Ankur Gupta, Rohit Pippara, Pramod Pal, and Adit . *Wireless Sensing Systems: A Review*, pages 143–192. 01 2019.

[33] Ankur Gupta, S. S. Pandey, Monalisha Nayak, Subhashish Basu Maity, Arnab andMajumder, and Shantanu Bhattacharya. Hydrogen sensing based on nanoporous silica-embedded ultra dense znonanobundles. *RSC Adv.*, 4:7476–7482, 2014.

[34] Ankur Gupta, Shubhra Gangopadhyay, Keshab Gangopadhyay, and shantanu Bhattacharya. Palladium-functionalized nanostructured platforms for enhanced hydrogen sensing. *Nanomaterials and Nanotechnology*, 6:40, 2016.

[35] Ankur Gupta. *Nano-energetic Materials for Defense Application*, pages 81–108. 11 2018.

[36] Gulshan Kumar Verma and Mohd. Zahid Ansari. Design and simulation of piezoresistive polymer accelerometer. *IOP Conference Series: Materials Science and Engineering*, 561:012128, nov 2019.

[37] C. B. Williams, A. Pavic, R. S. Crouch, and R. C. Woods. Feasibility Study of a Vibration-electric Generator for Bridge Vibration Sensors. In *Proceedings of the 16th International Modal Analysis Conference*, volume 3243 of *Society of Photo-Optical Instrumentation Engineers (SPIE) Conference Series*, page 1111, February 1998.

[38] Yanxin Zhuang, Ole Hansen, Thomas Knieling, Christian Wang, Pirmin Rombach, Walter Lang, Wolfgang Benecke, Markus Kehlenbeck, and Jörn Koblitz. Thermal stability of vapor phase deposited self-assembled monolayers for mems anti-stiction. *Journal of Micromechanics and Microengineering*, 16:2259, 09 2006.

[39] MJ Tudor, MV Andres, KWH Foulds, and JM Naden. Silicon resonator sensors: interrogation techniques and characteristics. *IEE Proc D*, 135(5), 1988.

[40] Shirin Ghaffari, Saurabh Chandorkar, Shasha Wang, Eldwin Ng, C.H. Ahn, V.A. Hong, Yushi Yang, and Thomas Kenny. Quantum limit of quality factor in silicon micro and nano mechanical resonators. *Scientific reports*, 3:3244, 11 2013.

[41] G.Q. Wu, D.H. Xu, B. Xiong, L.F. Che, and Y.L. Wang.

[42] Mohammmad H Hasan, Fadi Alsaleem, Nizar Jaber, Md Al Hafiz, and Mohammad Younis. Simultaneous electrical and mechanical resonance drive for large signal amplification of micro resonators. *AIP Advances*, 8:015312, 01 2018.

[43] J. Lu, T. Ikehara, Y. Zhang, T. Mihara, T. Itoh, and R. Maeda. High quality factor silicon cantilever driven by pzt actuator for resonant based mass detection. In *2008 Symposium on Design, Test, Integration and Packaging of MEMS/MOEMS*, pages 60–65, 2008.

[44] G Stemme. Resonant silicon sensors. *Journal of Micromechanics and Microengineering*, 1(2):113–125, jun 1991.

[45] K.Y. Yasumura, T.D. Stowe, E.M. Chow, T. Pfafman, T.W. Kenny, B.C. Stipe, and D. Rugar. Quality factors in micron- and submicron-thick cantilevers. *Journal of Microelectromechanical Systems*, 9(1):117–125, 2000.

[46] Ashwin K. Samarao and Farrokh Ayazi. Temperature compensation of silicon resonators via degenerate doping. *IEEE Transactions on Electron Devices*, 59(1):87–93, 2012.

[47] N Heidrich, D Iankov, J Hees, W Pletschen, R E Sah, L irste, V Zuerbig, C Nebel, O Ambacher, and V Lebedev. Enhanced mechanical performance of AlN/nanodiamond micro-resonators. *Journal of Micromechanics and Microengineering*, 23(12):125017, nov 2013.

[48] Ross G. Turnbull, Mike C. L. Ward, Steve Collins, and Carl J. Anthony. A simple technique to increase the quality factor of micro-mechanical resonators. In Thomas George, M. Saif Islam, and Achyut K. Dutta, editors, *Micro- and Nanotechnology Sensors, Systems, and Applications*, volume 7318, pages 369 – 376. International Society for Optics and Photonics, SPIE, 2009.

[49] Ilkka Tittonen and Mika Koskenvuori. pages 294–312. Elsevier Inc., United States, 2 edition, jan 2015.

[50] Arash Hajjam, Amir Rahafrooz, and Siavash Pourkamali. Temperature compensated single-device electromechanicaloscillators. *Proceedings of the IEEE International Conference on Micro Electromechanical Systems (MEMS)*, pages 801–804, 01 2011.

[51] J. R. Clark, W. Hsu, and C. Nguyen. High-q vhf micromechanical contour-mode disk resonators. *International Electron Devices Meeting 2000.TechnicalDigest. IEDM (Cat. No.00CH37138)*, pages 493–496, 2000.

[52] Arash Hajjam, Amir Rahafrooz, and Siavash Pourkamali. Sub-100ppb/degrees c temperature stability in thermally actuated high frequency silicon resonators via degenerate phosphorous doping and bias current optimization. pages 7.5.1 – 7.5.4, 01 2011.

[53] R. Abdolvand and F. Ayazi. 7e-4 enhanced power handling and quality factor in thin-film piezoelectric-on-substrate resonators. *2007 IEEE Ultrasonics Symposium Proceedings*, pages 608–611, 2007.

[54] K. Ekinci, Ya Tang Yang, and Michael Roukes. Ultimate limits to inertial mass sensing based upon nanoelectromechanical systems. *Journal of Applied Physics*, 95, 09 2003.

[55] Amit Banerjee, Nitul S. Rajput, and S. S. Banerjee. Unusual dimensional dependence of resonance frequencies of au nanocantilevers fabricated with self-organized microstructure. *AIP Advances*, 2(3):032105, 2012.

[56] J. L. Arlett, J. R. Maloney, B. Gudlewski, M. Muluneh, and M. L. Roukes. Self-sensing micro- and nanocantilevers with attonewton-scale force resolution. *Nano Letters*, 6(5):1000–1006, 2006.

[57] T. P. Burg and S. R. Manalis. Suspended microchannel resonators for biomolecular detection. *Applied Physics Letters*, 83(13):2698–2700, 2003.

[58] Giancarlo Canavese, Alessandro Ricci, Gian Carlo Gazzadi, Ivan Ferrante, Andrea Mura, Simone Marasso, and Carlo Ricciardi. Resonating behaviour of nanomachined holed microcantilevers. *Scientific Reports*, 5:17837, 12 2015.

[59] Lifang Niu, Jing Bo Zhang, Yuan Hsing Fu, Shripad Kulkarni, and Boris Lukyànchuk. Fano resonance in dual-disk ring plasmonic nanostructures. *Opt. Express*, 19(23):22974–22981, Nov 2011.

[60] Arthur T. Zielinski, Abhinav Prasad, Ashwin A. Seshia, Markus Kalberer, and Roderic L. Jones. Effects of spatial sensitivity on mass sensing with bulk acoustic mode resonators. *Sensors and Actuators A: Physical*, 236:369–379, 2015.

[61] Angel T-H. Lin, Jize Yan, and Ashwin A. Seshia. Mechanically coupled bulk-mode dual resonator mass sensor. *Procedia Engineering*, 5:1454–1457, 2010. Eurosensor XXIV Conference.

[62] Cheng Tu, Haoshen Zhu, Yuanjie Xu, and Joshua E.-Y. Lee. Differential-capacitive-input and differential-piezoresistive-output enhanced transduction of a silicon bulk-mode microelectromechanical resonator. *Sensors and Actuators A: Physical*, 210:41–50, 2014.

[63] Ville Kaajakari, Tomi Mattila, Aarne Oja, Jyrki Kiihamäki, and Heikki Seppä. Square-extensional mode single-crystal silicon micromechanical resonator for low-phase-noise oscillator applications. *Electron Device Letters, IEEE*, 25:173 – 175, 05 2004.

[64] Gavin K. Ho, Reza Abdolvand, Abhishek Sivapurapu, Shweta Humad, and Farrokh Ayazi. Piezoelectric-on-silicon lateral bulk acoustic wave micromechanical resonators. *Journal of Microelectromechanical Systems*, 17(2):512–520, 2008.

[65] M. Maqueda López, M. Fernandéz-Bolaños Badía, W. Vitale, and A.M. Ionescu. Solid-gap wine-glass mode disks vb-fet resonators applied to biomass sensing. *Microelectron. Eng.*, 145(C):53–57, September 2015.

[66] Marc-Alexandre Dubois and Claude Muller. *Thin-Film Bulk Acoustic Wave Resonators*, pages 3–28. 07 2013.

[67] Bertrand Dubus. Future trends in acoustic rf mems devices. In *MEMS-based circuits and systems for wirelesscommunication*, pages 95–117. Springer, 2013.

[68] Zdravko Stanimirović and Ivanka Stanimirović. Mechanical properties of mems materials. In Kenichi Takahata, editor, *Micro Electronic and Mechanical Systems*, chapter 11. IntechOpen, Rijeka, 2009.

[69] Zahid Mehmood, Ibraheem Haneef, and Florin Udrea. Material selection for micro-electro-mechanical-systems (mems) using ashby's approach. *Materials & Design*, 157:412–430, 2018.

[70] Xiaofeng Zhao, Ying Wang, and Dianzhong Wen. Fabrication and characteristics of a soi three-axis acceleration sensor based on mems technology. *Micromachines*, 10(4), 2019.

[71] Pasqualina M Sarro. Silicon carbide as a new mems technology. *Sensors and Actuators A: Physical*, 82(1):210–218, 2000.

[72] Ankur Gupta and Pramod Pal. *Flexible Sensors for Biomedical Application*, pages 287–314. 12 2018.

[73] Yook-Kong Yong, Mihir Patel, and Masako Tanaka. Estimation of quartz resonator q and other figures of merit by an energy sink method. *Ultrasonics, Ferroelectrics and Frequency Control, IEEETransactions on*, 54:1386 – 1398, 08 2007.

[74] Rudra Pratap and A Arunkumar. Material selection for mems devices. 2007.

[75] Fabricating mems and nanotechnology. `https://www.memsnet.org/about/fabrication.html.`, 2020.

[76] Sangwoo Lee, Sangjun Park, and D.-I. Cho. The surface/bulk micromachining (sbm) process: a new method for fabricating released mems in single crystal silicon. *Journal of Microelectromechanical Systems*, 8(4):409–416, 1999.

[77] E Gentili, L Tabaglio, and F Aggogeri. Review on micromachining techniques. In *AMST'05 advanced manufacturing systems andtechnology*, pages 387–396. Springer, 2005.

[78] Wanling Pan, Philippe Soussan, Bart Nauwelaers, and Harrie A.C. Tilmans. A surface micromachined electrostatically tunable film bulk acoustic resonator. *Sensors and Actuators A: Physical*, 126(2):436–446, 2006.

[79] Azrul Azlan Hamzah, Jumril Yunas, Burhanuddin Yeop Majlis, and Ibrahim Ahmad. Sputtered encapsulation as wafer level packaging for isolatable mems devices: A technique demonstrated on a capacitive accelerometer. *Sensors*, 8(11):7438–7452, 2008.

[80] Bao Q. Ta, Tormod B. Haugen, Nils Hoivik, Einar Halvorsen, and Knut E. Aasmundtveit. Local synthesis of carbon nanotubes in silicon microsystems: The effect of temperature distribution on growth structure. *Materials*, 6(8):3160–3170, 2013.

[81] R.T. Howe. Applications of silicon micromachining to resonator fabrication. In *Proceedings of IEEE 48th Annual Symposium on Frequency Control*, pages 2–7, 1994.

[82] Frederic Nabki, Paul-Vahé Cicek, Tomas A. Dusatko, and Mourad N. El-Gamal. Low-stress cmos-compatible silicon carbide surface-micromachining technology—part ii: Beam resonators for mems above ic. *Journal of Microelectromechanical Systems*, 20(3):730–744, 2011.

[83] William P Eaton, James H Smith, David J Monk, Gary OBrien, and Todd F Miller. Comparison of bulk-and surface-micromachined pressure sensors. Technical report, Sandia National Labs., Albuquerque, NM (United States), 1998.

[84] Zachary J. Davis, Winnie Svendsen, and Anja Boisen. Design, fabrication and testing of a novel mems resonator for mass sensing applications. *Microelectronic Engineering*, 84(5):1601–1605, 2007. Proceedings of the 32nd International Conference on Micro- and Nano-Engineering.

[85] Christian Rusch, Martin Börner, Jürgen Mohr, Thomas Zwick, Yi Chen, and Héctor J. De Los Santos. Electrical tuning of dielectric resonators with liga-mems. In *2013 European Microwave Integrated Circuit Conference*, pages 316–319, 2013.

[86] Abolfazl Bijari, S. H. Keshmiri, Winai Wanburee, Ch Sriphung, and Rungrueang Phatthanakun. Design and fabrication of a narrow-bandwidth micromechanical ring filter using a novel process in uv-liga technology. *Iranian Journal of Electrical and Electronic Engineering*, 8:280–289, 12 2012.

[87] Js Kim, Yb Ko, Chul Hwang, Jong Kim, and Kyungho Yoon. Fabrication of micro injection mold with modified liga micro-lens pattern and its application to lcd-blu. *Korea Australia Rheology Journal*, 19:165–169, 11 2007.

[88] J. Hormes, J. Göttert, K. Lian, Y. Desta, and L. Jian. Materials for liga and liga-based microsystems. *Nuclear Instruments and Methods in Physics Research Section B: Beam Interactions with Materials and Atoms*, 199:332–341, 2003.

[89] Rajeev Singh, Avinash Kumar, Rishi Kant, Ankur Gupta, Suresh Ellappan, and Shantanu Bhattacharya. Design and fabrication of 3-dimensional helical structures in polydimethylsiloxane for flow control applications. *Microsystem Technologies*, 20, 01 2014.

[90] AA Istratov, H Hieslmair, and ER Weber. Iron contamination in silicon technology. *Applied Physics A*, 70(5):489–534, 2000.

[91] Gaurav Gupta, R.K. Tyagi, S.K. Rajput, Palaash Saxena, Anugrah Vashisth, and Sarthak Mehndiratta. Pvd based thin film deposition methods and characterization / property of different compositional coatings - a critical analysis. *Materials Today: Proceedings*, 38:259–264, 2021. 2nd International Conference on Future Learning Aspects of Mechanical Engineering.

[92] L. García-Gancedo, Z.Zhu Zhu, Enrique Iborra, Marta Clement, Jimena Olivares, A.J. Flewitt, W. Milne, Gregory Ashley, Xiubo Zhao, and Jian Lu. Aln-based baw resonators with cnt electrodes for gravimetric biosensing. *Sensors and Actuators B Chemical*, B160:1386, 12 2011.

[93] Ankur Gupta, Geeta Bhatt, and Shantanu Bhattacharya. Novel dipstick model for portable bio-sensing application. 7:36–41, 04 2019.

[94] Motoaki Hara, Jan Kuypers, Takashi Abe, and Masayoshi Esashi. Surface micromachined aln thin film 2ghz resonator for cmos integration. *Sensors and Actuators A: Physical*, 117(2):211–216, 2005.

[95] Ankur Gupta, Poonam Sundriyal, Aviru Basu, Kapil Manoharan, Rishi Kant, and Shantanu Bhattacharya. Nano-finishing of mems-based platforms for optimum optical sensing. *Journal of Micromanufacturing*, 3:251659841986267, 11 2019.

[96] Matthew A Hopcroft. *Temperature-stabilized silicon resonators for frequency references*. ProQuest, 2007.

[97] Pankaj Singh Chauhan, Ashutosh Rai, Ankur Gupta, and Shantanu Bhattacharya. Enhanced photocatalytic performance of vertically grown ZnO nanorods decorated with metals (al, ag, au, and au–pd) for degradation of industrial dye. *Materials Research Express*, 4(5):055004, may 2017.

[98] H Hoche, C Rosenkranz, A Delp, MM Lohrengel, E Broszeit, and C Berger. Investigation of the macroscopic and microscopic electrochemical corrosion behaviour of pvd-coated magnesium die cast alloy az91. *Surface and Coatings Technology*, 193(1-3):178–184, 2005.

[99] Elbert Contreras Romero, Abel Hurtado Macías, Juan Méndez Nonell, Oscar Solís Canto, and Maryory Gómez Botero. Mechanical and tribological properties of nanostructured tialn/tan coatings deposited by dc magnetron sputtering. *Surface and Coatings Technology*, 378:124941, 2019.

[100] Harish C. Barshilia, B. Deepthi, and K.S. Rajam. Growth and characterization of aluminum nitride coatings prepared by pulsed-direct current reactive unbalanced magnetron sputtering. *Thin Solid Films*, 516(12):4168–4174, 2008.

[101] A. Ababneh, U. Schmid, J. Hernando, J.L. Sánchez-Rojas, and H. Seidel. The influence of sputter deposition parameters on piezoelectric and mechanical properties of aln thin films. *Materials Science and Engineering: B*, 172(3):253–258, 2010.

[102] A.U. Chaudhry, Bilal Mansoor, Tarang Mungole, Georges Ayoub, and David P. Field. Corrosion mechanism in pvd deposited nano-scale titanium nitride thin film with intercalated titanium for protecting the surface of silicon. *Electrochimica Acta*, 264:69–82, 2018.

[103] Mariana Fraga and Rodrigo Pessoa. Progresses in synthesis and application of sic films: From cvd to ald and from mems to nems. *Micromachines*, 11(9), 2020.

[104] Thura Lin Naing. *Capacitive-Gap MEMS Resonator-Based Oscillator Systems for Low-Power Signal Processing.* University of California, Berkeley, 2015.

[105] James J Allen. *Micro electro mechanical system design.* CRC press, 2005.

[106] E. Serra, M. Bonaldi, A. Borrielli, L. Conti, G. Pandraud, and P.M. Sarro. Selective coating deposition on high-q single-crystal silicon resonators for the investigation of thermal noise statistical properties.

Procedia Engineering, 87:1485–1488, 2014. EUROSENSORS 2014, the 28th European Conference on Solid-State Transducers.

[107] S. Sedky, P. Fiorini, M. Caymax, S. Loreti, K. Baert, L. Hermans, and R. Mertens. Structural and mechanical properties of polycrystalline silicon germanium for micromachining applications. *Journal of Microelectromechanical Systems*, 7(4):365–372, 1998.

[108] P.M. Sarro, C.R. deBoer, E. Korkmaz, and J.M.W. Laros. Low-stress pecvd sic thin films for ic-compatible microstructures. *Sensors and Actuators A: Physical*, 67(1):175–180, 1998.

[109] D. Joachim and Liwei Lin. Characterization of selective polysilicon deposition for mems resonator tuning. *Journal of Microelectromechanical Systems*, 12(2):193–200, 2003.

[110] Avinash Kumar, Ankur Gupta, Nadeem Akhtar, Nachiketa Tiwari, Janakarajan Ramkumar, Shantanu Bhattacharya, and Rishi Kant. Optimization of laser machining process for the preparation of photomasks, and its application to microsystems fabrication downloaded from: http://nanolithography.spiedigitallibrary.org/ on 05/12/2015 terms of use: http://spiedl.org/terms optimization of laser machining process for the preparation of photomasks, and its application to microsystems fabrication. 01 2013.

[111] L. Mosher, B. Morgan, C.M. Waits, and R. Ghodssi. Advanced techniques in 3d photolithography for mems. page 6, 11 2006.

[112] Pengcheng Yan, Yulan Lu, Chao Xiang, Junbo Wang, Deyong Chen, and Jian Chen. A temperature-insensitive resonant pressure micro sensor based on silicon-on-glass vacuum packaging. *Sensors*, 19(18), 2019.

[113] J.W. Coburn. Pattern transfer. *Superlattices and Microstructures*, 2(1):17–25, 1986.

[114] Sami Franssila and Santeri Tuomikoski. *MEMS Lithography*, pages 333–348. 12 2010.

[115] Prasanna Deshpande, Rajesh Pande, and Rajendra Patrikar. Fabrication and characterization of zinc oxide piezoelectric mems resonator. *Microsystem Technologies*, 26:415–423, 02 2020.

[116] Ferran Martín and Jordi Bonache. Application of rf-mems-based split ring resonators (srrs) to the implementation of reconfigurable stopband filters: A review. *Sensors (Basel, Switzerland)*, 14:22848–22863, 12 2014.

[117] Zhenyu Luo, Deyong Chen, Junbo Wang, Yinan Li, and Jian Chen. A high-q resonant pressure microsensor with through-glass electrical interconnections based on wafer-level mems vacuum packaging. *Sensors (Basel, Switzerland)*, 14:24244–24257, 12 2014.

[118] Chien-Hao Weng, Gayathri Pillai, and Sheng-Shian Li. A thin-film piezoelectric-on-silicon mems oscillator for mass sensing applications. *IEEE Sensors Journal*, 20(13):7001–7009, 2020.

[119] Kazuaki Tanaka, Ryuji Kihara, Ana Sánchez-Amores, Josep Montserrat, and Jaume Esteve. Parasitic effect on silicon mems resonator model parameters. *Microelectronic Engineering*, 84(5):1363–1368, 2007. Proceedings of the 32nd International Conference on Micro- and Nano-Engineering.

[120] Markku Tilli, Mervi Paulasto-Kröckel, Matthias Petzold, Horst Theuss, Teruaki Motooka, and Veikko Lindroos. *Handbook of silicon based MEMS materials and technologies*. Elsevier, 2020.

[121] S Negi and R Bhandari. Silicon isotropic and anisotropic etching for mems applications. *Microsystem technologies*, 19(2):203–210, 2013.

[122] Xiaohui Du, Liying Wang, Anlin Li, Lingyun Wang, and Daoheng Sun. High accuracy resonant pressure sensor with balanced-mass detf resonator and twinborn diaphragms. *Journal of Microelectromechanical Systems*, 26(1):235–245, 2017.

[123] M. Aslam. Bulk etching of silicon wafer and development of a polyimide membrane. *Journal of Physics Conference Series*, 439:2029–, 06 2013.

[124] D. Kauzlarick. Fundamentals of microfabrication, the science of miniaturization, 2nd edition [book review]. *Engineering in Medicine and Biology Magazine, IEEE*, 22:109– 111, 04 2003.

[125] Prem Pal and Kazuo Sato. Fabrication methods based on wet etching process for the realization of silicon mems structures with new shapes. *Microsystem Technologies*, 16:1165–1174, 07 2010.

[126] Paul Hammond. Vapor-phase etch processes for silicon mems. In *Handbook of Silicon Based MEMS Materials and Technologies*, pages 519–530. Elsevier, 2020.

[127] Sheng-Shian Li and Shyam Trivedi. Cmos-mems resonant transducers for frequency control and sensing. In *2020 IEEE 33rd International Conference on Micro Electro Mechanical Systems (MEMS)*, pages 176–181, 2020.

[128] Etching processes. `https://www.mems-exchange.org/MEMS/processes/etch.html.`, 2020.

[129] Harmeet Bhugra and Gianluca Piazza. *Piezoelectric MEMS resonators*. Springer, 2017.

[130] Chupong Pakpum and Nirut Pussadee. Design of experiments for (100) si vertical wall wet etching using sonicated naoh solution. *Applied Mechanics and Materials*, 804:12–15, 10 2015.

[131] Avvaru Narasimha Rao, Swarnalatha Veerla, and Prem Pal. Etching characteristics of si110 in 20 wthydroxylamine for the fabrication of bulk micromachined mems. *Micro and Nano Systems Letters*, 5, 12 2017.

[132] Ivo Rangelow. Dry etching-based silicon micro-machining for mems. *Vacuum*, 62:279–291, 06 2001.

[133] Manish Hooda, Manoj Wadhwa, Sanjay Verma, M.M. Nayak, P.J. George, and A. Paul. A systematic study of drie process for high aspect ratio microstructuring. *Vacuum*, 84:1142–1148, 04 2010.

[134] Julien Arcamone, Gemma Rius, Gabriel Abadal, Jordi Teva, Nuria Barniol, and Francesc Pérez-Murano. Micro/nanomechanical resonators for distributed mass sensing with capacitive detection. *Microelectronic Engineering*, 83(4):1216–1220, 2006. Micro- and Nano-Engineering MNE 2005.

[135] V. Kaajakari, J. Kiihamaki, A. Oja, H. Seppa, S. Pietikainen, V. Kokkala, and H. Kuisma. Stability of wafer level vacuum encapsulated single-crystal silicon resonators. In *The 13th International Conference on Solid-State Sensors, Actuators and Microsystems, 2005. Digest of Technical Papers. TRANSDUCERS '05.*, volume 1, pages 916–919 Vol. 1, 2005.

[136] Takashi Abe and Yousuke Itasaka. A fabrication method of high-q quartz crystal resonator using double-layered etching mask for drie. *Sensors and Actuators A: Physical*, 188:503–506, 2012. Selected papers from The 16th International Conference on Solid-State Sensors, Actuators and Microsystems.

[137] Graham S. Wood, Chun Zhao, Suan Hui Pu, Stuart A. Boden, Ibrahim Sari, and Michael Kraft. Mass sensor utilising the mode-localisation effect in an electrostatically-coupled mems resonator pair fabricated using an soi process. *Microelectronic Engineering*, 159:169–173, 2016. Micro/Nano Devices and Systems 2015.

[138] Jiacheng Liu, Temesgen Workie, Ting Wu, Zhaohui Wu, Keyuan Gong, and Ken-ya Hashimoto. Q-factor enhancement of thin-film piezoelectric-on-silicon mems resonator by phononic crystal-reflector composite structure. *Micromachines*, 11:1130, 12 2020.

[139] Yulan Lu, Yan Pengcheng, Chao Xiang, Deyong Chen, Junbo Wang, Bo Xie, and Jian Chen. A resonant pressure microsensor with the measurement range of 1 mpa based on sensitivities balanced dual resonators. *Sensors*, 19:2272, 05 2019.

[140] Xiangguang Han, Qi Mao, Libo Zhao, Xuejiao Li, Li Wang, Ping Yang, Dejiang Lu, Yonglu Wang, Xin Yan, Songli Wang, et al. Novel resonant pressure sensor based on piezoresistive detection and symmetrical in-plane mode vibration. *Microsystems & Nanoengineering*, 6(1):1–11, 2020.

[141] Mems gas flow sensor based on thermally induced cantilever resonance frequency shift. *IEEE Sensors Journal*, 20(8):4139–4146, 2020.

[142] Xiaoqing Shi, Sen Zhang, Deyong Chen, Junbo Wang, Jian Chen, Bo Xie, Yulan Lu, and Yadong Li. A resonant pressure sensor based

upon electrostatically comb driven and piezoresistively sensed lateral resonators. *Micromachines*, 10(7), 2019.

[143] F. Kuo, C. Y. Lin, P. Chuang, C. Chien, Y. Yeh, and Stella K. A. Wen. Monolithic multi-sensor design with resonator-based mems structures. *IEEE Journal of the Electron Devices Society*, 5:214–218, 2017.

[144] Chong-Yang Lin and Kuei-Ann Wen. Mems resonator based thermometer soc design in cmos 0.18 μm standard process. In *2016 International SoC Design Conference (ISOCC)*, pages 13–14. IEEE, 2016.

[145] S.H. Tseng, Y.T. Hsieh, C.C. Lin, H.H. Tsai, and Y.Z. Juang. Cmos mems resonator oscillator with an on-chip boost dc/dc converter. In *2015 Transducers - 2015 18th International Conference on Solid-State Sensors, Actuators and Microsystems (TRANSDUCERS)*, pages 1981–1984, 2015.

[146] Vivek Garg, Rakesh Mote, and Jing Fu. Facile fabrication of functional 3d micro-nano architectures with focused ion beam implantation and selective chemical etching. *Applied Surface Science*, 526:146644, 05 2020.

[147] F. Watt, Andrew Bettiol, Jeroen van Kan, Ee Jin Teo, and Mark Breese. Ion beam lithography and nanofabrication: A review. *International Journal of Nanoscience*, 4:269 – 286, 06 2005.

[148] Zhuang Xiong, B Walter, E Mairiaux, Marc Faucher, Lionel Buchaillot, and B Legrand. Mems piezoresistive ring resonator for afm imaging with pico-newton force. *Journal of Micromechanics and Microengineering*, 23:035016, 01 2013.

[149] Chengli Wang, Chen Shen, Ailun Yi, Shumin Yang, Liping Zhou, Yifan Zhu, Kai Huang, Sannian Song, Min Zhou, Jiaxiang Zhang, and Xin Ou. Visible and near-infrared microdisk resonators on a 4h-silicon-carbide-on-insulator platform, 03 2021.

[150] V Cimalla, Joerg Pezoldt, and Oliver Ambacher. Group iii nitride and sic based mems and nems: Materials properties, technology and applications. *J. Phys. D: Appl. Phys*, 40:6386–6434, 10 2007.

[151] K. Brueckner, Florentina Gannott, Katja Tonisch, Christian Förster, Volker Cimalla, R. Stephan, Joerg Pezoldt, Thomas Stauden, Oliver Ambacher, and Matthias Hein. Micro- and nano-electromechanical resonators based on sic and group iii-nitrides for sensor applications. *Fraunhofer IAF*, 208, 02 2011.

[152] Seong Chan Jun, X. Huang, M. Manolidis, Christian Zorman, Mehran Mehregany, and James Hone. Electrothermal tuning of al-sic nanomechanical resonators. *Nanotechnology*, 17:1506 –1511, 03 2006.

[153] A. Magyar, D. O. Bracher, J. Lee, I. Aharonovich, and E. Hu. High quality sic microdisk resonators fabricated from monolithic epilayer wafers. *Applied Physics Letters*, 104:051109, 2014.

[154] Philipp Koehn. Neural machine translation. 09 2017.

[155] JTM Van Beek and Rob Puers. A review of mems oscillators for frequency reference and timing applications. *Journal of Micromechanics and Microengineering*, 22(1):013001, 2011.

[156] Guoqiang Wu, Dehui Xu, Bin Xiong, Yuchen Wang, Yuelin Wang, and Yinglei Ma. Wafer-level vacuum packaging for mems resonators using glass frit bonding. *Journal of microelectromechanical systems*, 21(6):1484–1491, 2012.

[157] Janna Rodriguez, Saurabh A Chandorkar, Christopher A Watson, Grant M Glaze, CH Ahn, Eldwin J Ng, Yushi Yang, and Thomas W Kenny. Direct detection of akhiezer damping in a silicon mems resonator. *Scientific reports*, 9(1):1–10, 2019.

[158] C.B. O'Neal, A.P. Malshe, S.B. Singh, William Brown, and W.P. Eaton. Challenges in the packaging of mems. pages 41 – 47, 04 1999.

[159] Muhammad Shoaib, Nor Hisham Hamid, Aamir Farooq Malik, Noohul Basheer Zain Ali, and Mohammad Tariq Jan. A review on key issues and challenges in devices level mems testing. *Journal of Sensors*, 2016, 2016.

[160] Jin Xie. Fabrication challenges and test structures for high-aspect-ratio soi mems devices with refilled electrical isolation trenches. *Microsyst. Technol.*, 21(8):1719–1727, August 2015.

[161] YP Zhao, L. Wang, and T. Yu. Mechanics of adhesion in mems - a review. *J. Adhesion Sci. Technol*, 17:519–546, 01 2003.

[162] P. Verma, K. Z. Khan, S. Fomchenkov, and R. Gopal. Su-8 based uv-liga fabrication process for realization of nickel based mems inertial sensor. In *ICIT 2016*, 2016.

[163] Ali Kourani, Emad Hegazi, and Yehea Ismail. Electronic frequency compensation of aln-on-si mems reference oscillators. *Microelectronics Journal*, 54:72–84, 2016.

[164] Iraj S. Amiri, M. M. Ariannejad, S. Daud, and P. Yupapin. High sensitive temperature sensor silicon-based microring resonator using the broadband input spectrum. *Results in Physics*, 9:1578–1584, jun 2018.

[165] Kenji Okabe, Wang-Hoon Lee, Yasoo Harada, and Makoto Ishida. Silicon based on-chip antenna using an lc resonator for near-field rf systems. *Solid-State Electronics*, 67:100–104, 01 2012.

[166] Libo Zhao, Linya Huang, Guoxi Luo, Jiuhong Wang, Hongyan Wang, Yongshun Wu, Zhikang Li, Xiangyang Zhou, and Zhuangde Jiang. An immersive resonant sensor with microcantilever for pressure measurement. *Sensors and Actuators A: Physical*, 303:111686, 2020.

[167] Sadaf Charkhabi, Yee Jher Chan, Subhanwit Roy, Md Monirul Islam, Brock B. Duffield, Kyle J. Jackson, Lujia Bu, Sang-Hwan Kim, Andrew C. Hillier, Nathan M. Neihart, and Nigel F. Reuel. Effects of fabrication materials and methods on flexible resonant sensor signal quality. *Extreme Mechanics Letters*, 41:101027, 2020.

[168] Denis DEZEST, Fabrice Mathieu, Laurent Mazenq, Caroline Soyer, Jean Costecalde, D. Remiens, Jean-François Deü, and Liviu Nicu. Wafer-scale fabrication of self-actuated piezoelectric nanoelectromechanical resonators based on lead zirconate titanate (pzt). *Journal of Micromechanics and Microengineering*, 25, 03 2015.

[169] Shujing Su, Fei Lu, Guozhu Wu, Dezhi Wu, Qiulin Tan, Helei Dong, and Jijun Xiong. Slot antenna integrated re-entrant resonator based wireless pressure sensor for high-temperature applications. *Sensors*, 17(9), 2017.

[170] Luca Belsito, M. Ferri, Fulvio Mancarella, Luca Masini, Jize Yan, Ashwin Seshia, Kenichi Soga, and Alberto Roncaglia. Fabrication of high-resolution strain sensors based on wafer-level vacuum packaged mems resonators. *Sensors and Actuators A: Physical*, 239, 01 2016.

[171] C Ciminelli, F Dell'Olio, D Conteduca, CM Campanella, and MN Armenise. High performance soi microring resonator for biochemical sensing. *Optics & laser technology*, 59:60–67, 2014.

[172] Marko Bakula, Frederik Ceyssens, and Robert Puers. A mems resonator as a power receiver for inductively powered implantable sensors. *Procedia Engineering*, 120:570–573, 12 2015.

[173] Zhengxiang Fang, Yonggang Yin, Xiaofei He, Fengtian Han, and Yunfeng Liu. Temperature-drift characterization of a micromachined resonant accelerometer with a low-noise frequency readout. *Sensors and Actuators A: Physical*, 300:111665, 2019.

[174] Xianhao Le, Li Peng, Jintao Pang, Zhen Xu, Chao Gao, and Jin Xie. Humidity sensors based on aln microcantilevers excited at high-order resonant modes and sensing layers of uniform graphene oxide. *Sensors and Actuators B: Chemical*, 283:198–206, 2019.

[175] Qiangxian Huang, Yang Zhao, Dan Yuan, Liansheng Zhang, and Zhenying Cheng. Characteristics of a dynamic atomic force microscopy based on a higher-order resonant silicon cantilever and experiments. *Measurement*, 94:31–36, 2016.

[176] Sagnik Ghosh and Joshua Lee. A lorentz force magnetometer based on a piezoelectric-on-silicon square-extensional mode micromechanical resonator. *Applied Physics Letters*, 110:253507, 06 2017.

[177] Mustafa Yilmaz, Yasin Kilinc, Gokhan Nadar, Zuhal Tasdemir, Nicole Wollschläger, Werner Oesterle, Yusuf Leblebici, and B Erdem Alaca. Top-down technique for scaling to nano in silicon mems. *Journal of Vacuum Science & Technology B, Nanotechnology and Microelectronics: Materials, Processing, Measurement, and Phenomena*, 35(2):022001, 2017.

[178] Koji Sugano, Yuki Tanaka, Akio Uesugi, Etsuo Maeda, Reo Kometani, and Yoshitada Isono. Detection of wavelength shift of near-infrared

laser using mechanical microresonator-based sensor with si-covered gold nanorods as optical absorber. *Sensors and Actuators A: Physical*, 315:112337, 2020.

[179] Florian Patocka, Christoph Schneidhofer, Nicole Dörr, Michael Schneider, and Ulrich Schmid. Novel resonant mems sensor for the detection of particles with dielectric properties in aged lubricating oils. *Sensors and Actuators A: Physical*, 315:112290, 08 2020.

[180] Mohammad Mahdavi, Emad Mehdizadeh, and Siavash Pourkamali. Piezoelectric mems resonant dew point meters. *Sensors and Actuators A: Physical*, 276:52–61, 2018.

[181] Saeed Mohammadi, Ali. A. Eftekhar, Reza Pourabolghasem, and Ali Adibi. Simultaneous high-q confinement and selective direct piezoelectric excitation of flexural and extensional lateral vibrations in a silicon phononic crystal slab resonator. *Sensors and Actuators A: Physical*, 167(2):524–530, 2011. Solid-State Sensors, Actuators and Microsystems Workshop.

[182] Vassil Tzanov, Jordi Llobet, Francesc Torres, Francesc Perez-Murano, and Nuria Barniol. Multi-frequency resonance behaviour of a si fractal nems resonator. *Nanomaterials*, 10(4), 2020.

[183] Julien Philippe, Grégory Arndt, Eric Colinet, Mylène Savoye, Thomas Ernst, Eric Ollier, and Julien Arcamone. Fully monolithic and ultra-compact nems-cmos self-oscillator based-on single-crystal silicon resonators and low-cost cmos circuitry. In *2014 IEEE 27th International Conference on Micro Electro Mechanical Systems (MEMS)*, pages 1071–1074, 2014.

[184] Bo Li and Chengkuo Lee. Nems diaphragm sensors integrated with triple-nano-ring resonator. *Sensors and Actuators A: Physical*, 172(1):61–68, 2011. Eurosensors XXIV, Linz, Austria, 5-8 September 2010.

[185] Matteo Rinaldi, Chiara Zuniga, Brandon Duick, and Gianluca Piazza. Use of a single multiplexed cmos oscillator as direct frequency read-out for an array of eight aln contour-mode nems resonant sensors. *Departmental Papers (ESE)*, 11 2010.

[186] M. Rinaldi, C. Zuniga, C. Zuo, and G. Piazza. Ultra-thin super high frequency two-port aln contour-mode resonators and filters. In *TRANSDUCERS 2009 - 2009 International Solid-State Sensors, Actuators and Microsystems Conference*, pages 577–580, 2009.

[187] Mohammad Nasr Esfahani, Yasin Kilinc, M Çagatay Karakan, Ezgi Orhan, M Selim Hanay, Yusuf Leblebici, and B Erdem Alaca. Piezoresistive silicon nanowire resonators as embedded building blocks in thick soi. *Journal of Micromechanics and Microengineering*, 28(4):045006, 2018.

[188] A. Uranga, J. Verd, and N. Barniol. Cmos–mems resonators: From devices to applications. *Microelectronic Engineering*, 132:58–73, 2015. Micro and Nanofabrication Breakthroughs for Electronics, MEMS and Life Sciences.

[189] Reza Abdolvand, Behraad Bahreyni, Joshua E-Y Lee, and Frederic Nabki. Micromachined resonators: A review. *Micromachines*, 7(9):160, 2016.

[190] Chun Zhao, Mohammad H. Montaseri, Graham S. Wood, Suan Hui Pu, Ashwin A. Seshia, and Michael Kraft. A review on coupled mems resonators for sensing applications utilizing mode localization. *Sensors and Actuators A: Physical*, 249:93–111, 2016.

[191] Olebogeng Bone Kobe, Joseph Chuma, Rodrigo Jamisola Jr, and Matthews Chose. A review on quality factor enhanced on-chip microwave planar resonators. *Engineering Science and Technology, an International Journal*, 20(2):460–466, 2017.

[192] Liting Gai, Jin Li, and Yong Zhao. Preparation and application of microfiber resonant ring sensors: A review. *Optics & Laser Technology*, 89:126–136, 2017.

[193] Y. Tsaturyan, A. Barg, E. S. Polzik, and A. Schliesser. Ultracoherent nanomechanical resonators via soft clamping and dissipation dilution. *Nature Nanotechnology*, 12(8):776–783, 6 2017.

[194] Malika Tlili, Frédérique Deshours, Georges Alquié, Hamid Kokabi, Satria Hardinata, and Fabien Koskas. Microwave resonant sensor for

non-invasive characterization of biological tissues. *Irbm*, 39(6):445–450, 2018.

[195] Yuting Wang, Yao Pan, Tianliang Qu, Yonglei Jia, Kaiyong Yang, and Hui Luo. Decreasing frequency splits of hemispherical resonators by chemical etching. *Sensors*, 18(11), 2018.

[196] Saad Ilyas and Mohammad I Younis. Resonator-based m/nems logic devices: Review of recent advances. *Sensors and Actuators A: Physical*, 302:111821, 2020.

[197] Maria C Cardenosa-Rubio, Heather M Robison, and Ryan C Bailey. Recent advances in environmental and clinical analysis using microring resonator–based sensors. *Current opinion in environmental science & health*, 10:38–46, 2019.

[198] Amal Hajjaj, Nizar Jaber, Saad Ilyas, Feras Alfosail, and Mohammad Younis. Linear and nonlinear dynamics of micro and nano-resonators: Review of recent advances. *International Journal of Non-Linear Mechanics*, 119, 10 2019.

[199] Simone Berneschi, Francesca Bettazzi, Ambra Giannetti, Francesco Baldini, Gualtiero Nunzi Conti, Stefano Pelli, and Ilaria Palchetti. Optical whispering gallery mode resonators for label-free detection of water contaminants. *TrAC Trends in Analytical Chemistry*, 126:115856, 2020.

[200] Cheng Tu, Joshua E-Y Lee, and Xiao-Sheng Zhang. Dissipation analysis methods and q-enhancement strategies in piezoelectric mems laterally vibrating resonators: A review. *Sensors*, 20(17):4978, 2020.

[201] Gayathri Pillai and Sheng-Shian Li. Piezoelectric mems resonators: A review. *IEEE Sensors Journal*, pages 1–1, 2020.